

Water Resources Research®

RESEARCH ARTICLE

10.1029/2022WR032881

Alvise Finotello and Davide Tognin
contributed equally to this work.

Key Points:

- Effects of salt-marsh lateral erosion on the characteristics of tides and waves are investigated for the microtidal Venice Lagoon
- Salt-marsh loss primarily enhances mean high water levels and wave heights due to reduced friction and longer wind fetches
- Hydrodynamic changes depend on salt-marsh spatial distribution and elevation, as well as on the characteristics of tidal and wind forcings

Supporting Information:

Supporting Information may be found in the online version of this article.

Correspondence to:

A. Finotello and D. Tognin,
alvise.finotello@unipd.it;
davide.tognin@unipd.it

Citation:

Finotello, A., Tognin, D., Carniello, L., Ghinassi, M., Bertuzzo, E., & D'Alpaos, A. (2023). Hydrodynamic feedbacks of salt-marsh loss in the shallow microtidal back-barrier lagoon of Venice (Italy). *Water Resources Research*, 59, e2022WR032881. <https://doi.org/10.1029/2022WR032881>

Received 9 JUN 2022

Accepted 7 MAR 2023

Author Contributions:

Conceptualization: Alvise Finotello, Davide Tognin, Luca Carniello, Andrea D'Alpaos

Data curation: Alvise Finotello, Davide Tognin

Formal analysis: Alvise Finotello, Davide Tognin

© 2023. The Authors.

This is an open access article under the terms of the [Creative Commons Attribution License](https://creativecommons.org/licenses/by/4.0/), which permits use, distribution and reproduction in any medium, provided the original work is properly cited.

Hydrodynamic Feedbacks of Salt-Marsh Loss in the Shallow Microtidal Back-Barrier Lagoon of Venice (Italy)

Alvise Finotello^{1,2,3} , Davide Tognin^{2,4} , Luca Carniello^{2,4} , Massimiliano Ghinassi^{1,2}, Enrico Bertuzzo³ , and Andrea D'Alpaos^{1,2} 

¹Department of Geosciences, University of Padova, Padova, Italy, ²Center for Lagoon Hydrodynamics and Morphodynamics (C.I.Mo.La.), University of Padova, Padova, Italy, ³Department of Environmental Sciences, Informatics and Statistics, Ca' Foscari University of Venice, Venice, Italy, ⁴Department of Civil, Environmental, and Architectural Engineering, University of Padova, Padova, Italy

Abstract Extensive loss of salt marshes in back-barrier tidal embayments is ongoing worldwide as a consequence of land-use changes, wave-driven lateral marsh erosion, and relative sea-level rise compounded by mineral sediment starvation. However, how salt-marsh loss affects the hydrodynamics of back-barrier systems and feeds back into their morphodynamic evolution is still poorly understood. Here we use a depth-averaged numerical hydrodynamic model to investigate the feedback between salt-marsh erosion and hydrodynamic changes in the Venice Lagoon, a large microtidal back-barrier system in northeastern Italy. Numerical simulations are carried out for past morphological configurations of the lagoon dating back up to 1887, as well as for hypothetical scenarios involving additional marsh erosion relative to the present-day conditions. The progressive loss of salt marshes significantly impacted the lagoon hydrodynamics, both directly and indirectly, by amplifying high-tide water levels, reducing wind-wave energy dissipation, and critically affecting tidal asymmetries across the lagoon. Restoration projects and manmade protection of marsh margins, which have been implemented over the past few decades, limited the detrimental effects of marsh loss on the lagoon hydrodynamics, while not substantially changing the risk of flooding in urban lagoon settlements. Compared to previous studies, our analyses suggest that the hydrodynamic response of back-barrier systems to salt-marsh erosion is extremely site-specific, depending closely on the morphological characteristics of the embayment as well as on the external tidal and wind forcings.

1. Introduction

Tidal back-barrier lagoons represent critical environments at the interface between terrestrial, freshwater, and marine habitats (Flemming, 2012; Levin et al., 2001; Pérez-Ruzafa et al., 2019; Perillo, 1995), and are especially common along the World's coasts (Boothroyd et al., 1985; Fitzgerald & Hughes, 2019; Kjerfve, 1994; Stutz & Pilkey, 2011). They consist of sheltered embayments separated from the ocean by a system of barrier islands (Hesp, 2016) interrupted by tidal inlets (De Swart & Zimmerman, 2009). Back-barrier lagoons support high biodiversity, densely populated urban settlements, and florid economies (Barbier et al., 2011; Costanza et al., 1997; D'Alpaos & D'Alpaos, 2021). However, accelerating sea-level rise, reduced sediment supply, enhanced storminess, and increasing anthropogenic pressures exacerbate the threat to back-barrier lagoons and the communities relying on them (Gilby et al., 2021; Passeri et al., 2020). Although the current paradigm indicates that future coastal hazards will be mostly dictated by rising sea levels (Finkelstein & Ferland, 1987; González-Villanueva et al., 2015), previous studies demonstrated how geomorphological changes in tidal embayments can feedback into coastal hydrodynamics and enhance coastal hazards (Carniello et al., 2009; Ferrarin et al., 2015; Orton et al., 2020; Pollard et al., 2019; Ralston et al., 2019; Zhou et al., 2014). Therefore, investigating the feedback between geomorphological and hydrodynamic changes in back-barrier systems is of utmost importance to provide reliable assessments of coastal hazards (Carniello et al., 2009; Donatelli et al., 2018; Donatelli, Kalra, et al., 2020; Donatelli, Zhang, et al., 2020; Ferrarin et al., 2015; Vinet & Zhedanov, 2011; Zarzuelo et al., 2018).

Among the geomorphological features that characterize shallow back-barrier tidal embayments, salt marshes are especially common and provide a wide number of precious ecosystem services, including blue-carbon sequestration (Chmura et al., 2003), environmental remediation (Nelson & Zavaleta, 2012), shoreline protection (Möller et al., 2014; Temmerman et al., 2013), and habitat provision (Hopkinson et al., 2018; Pennings & He, 2021). The

Funding acquisition: Luca Carniello, Massimiliano Ghinassi, Enrico Bertuzzo, Andrea D'Alpaos
Investigation: Alvise Finotello, Davide Tognin
Methodology: Alvise Finotello, Davide Tognin
Project Administration: Andrea D'Alpaos
Software: Luca Carniello
Supervision: Alvise Finotello, Luca Carniello, Massimiliano Ghinassi, Enrico Bertuzzo, Andrea D'Alpaos
Validation: Alvise Finotello, Davide Tognin
Visualization: Davide Tognin
Writing – original draft: Alvise Finotello, Davide Tognin
Writing – review & editing: Alvise Finotello, Davide Tognin, Luca Carniello, Massimiliano Ghinassi, Enrico Bertuzzo, Andrea D'Alpaos

alarming rates of salt-marsh loss observed worldwide (Mcowen et al., 2017; Valiela et al., 2009) have prompted extensive studies on salt-marsh ecomorphodynamics (A. D'Alpaos et al., 2007; Fagherazzi et al., 2012; Finotello, D'Alpaos et al., 2022), as well as on the response of these ecosystems to changing hydrodynamic forcings and inorganic sediment supply (A. D'Alpaos et al., 2007; Finotello et al., 2020; Fitzgerald & Hughes, 2019; Gourgue et al., 2022; Hughes et al., 2021; Mariotti, 2020; Tommasini et al., 2019). In contrast, how salt-marsh loss affects hydrodynamics and the related morphodynamic evolution in shallow coastal bays still remains unclear. This uncertainty is mostly due to the paucity of study cases analyzed so far, thus calling for new insights into the feedback between salt-marsh loss and hydrodynamic changes in shallow back-barrier tidal systems (Donatelli et al., 2018; Donatelli, Zhang, et al., 2020; Silvestri et al., 2018; Vinet & Zhedanov, 2011).

Here we focus on the microtidal Venice Lagoon (Italy), where extensive marsh losses have been documented over the last two centuries (Carniello et al., 2009; L. D'Alpaos, 2010; Tommasini et al., 2019). We will pay particular attention to the feedback between wind-wave-induced salt-marsh erosion and changes in the lagoon hydrodynamics. The latter will be investigated using a custom-built, depth-averaged numerical model applied to several past morphological configurations of the Lagoon, each reconstructed based on available historical topographic and bathymetric maps. Moreover, exploratory simulations will be performed to unravel the hydrodynamic consequences of the failure to restore and protect salt marshes over the past few decades, which would have led to a further reduction in the total marsh extent compared to the present-day conditions.

2. Geomorphological Setting

Located in the northern Adriatic Sea, and characterized by an area of 550 km², the Venice Lagoon is the largest brackish waterbody in the Mediterranean Basin. The Lagoon formed over the last 7,500 years covering alluvial Late Pleistocene, silty-clayey deposits locally known as *Caranto* (Zecchin et al., 2008). The Lagoon's present-day morphology is characterized by the presence of three inlets, namely, from North to South: Lido, Malamocco, and Chioggia (Figures 1a–1d). Tides follow a semidiurnal microtidal regime, with a mean spring tidal range of 1 m and maximum tidal oscillations of about 0.75 m around Mean Sea Level (MSL) (e.g., D'Alpaos et al., 2013; Valle-Levinson et al., 2021).

Meteorological surges often overlap astronomical tides, thus producing significantly high (low) tides when atmospheric pressure is low (high). In addition, wind-related processes are critical for both the hydrodynamics and morphodynamics of the lagoon, with seasonal wind-storm events exerting a prominent morphodynamic control over decadal to centenary timescales (see Carniello et al., 2009, 2012). Detailed analyses of the wind climate show negligible interannual variability of wind energy (see Text S1 and Figure S1 in Supporting Information S1). The most morphologically and hydrodynamically meaningful wind-storm events are those associated with *Bora* and *Sirocco* winds (Figure 1e). The north-easterly *Bora* winds blow almost parallel to the major axis of the lagoon, thus producing pronounced water-level setups in the southern lagoon and generating large waves (significant wave height $H_s > 1$ m). Such waves promote significant resuspension of sediments from the tidal mudflats. In contrast, *Sirocco* winds blow from the South-East and cause large water-level setups in the northern Adriatic Sea, often leading to extensive flooding of Venice city and other settlements within the lagoon.

Over the last centuries, the hydrodynamics of the lagoon was severely affected by anthropogenic interventions (L. D'Alpaos, 2010; Ferrarin et al., 2015). First, by the end of the sixteenth century, all the major rivers debouching into the lagoon were diverted into the open sea, thus almost completely eliminating fluvial sediment input. Second, between the 1900s and 1970s, extensive land reclamation projects were carried out, especially along the landward margin of the lagoon, thus importantly reducing the total area open to the propagation of tides (see Figure 2). During the same period, the extraction of groundwater and natural gas for industrial purposes significantly accelerated the natural rates of soil subsidence (Carbognin et al., 2004; Gatto & Carbognin, 1981; Zanchettin et al., 2021). Moreover, in order to allow for increasingly bigger ships to cruise within the lagoon, two large waterways, namely the Vittorio Emanuele and the Malamocco-Marghera channels (Figures 2c and 2d), were excavated in 1925 and 1968, respectively. Major changes in the lagoon hydrodynamics were due to the construction of jetties at the lagoon inlets aimed to ensure water depths suitable for commercial ship traffic (Figures 1b–1d and Figures 2a–2d). The jetties at the Malamocco inlet were constructed between 1839 and 1872, whereas at the Lido inlet the northern jetty was completed in 1887 (see Figure 2a), with the southern jetty added later in 1892 (see Figure 2b). Finally, the jetties at the Chioggia inlet were built between 1910 and 1934 (Figure 2c). On the one hand, the jetties reduced the width of the inlets, thus resulting in considerable deepening as foreseen during

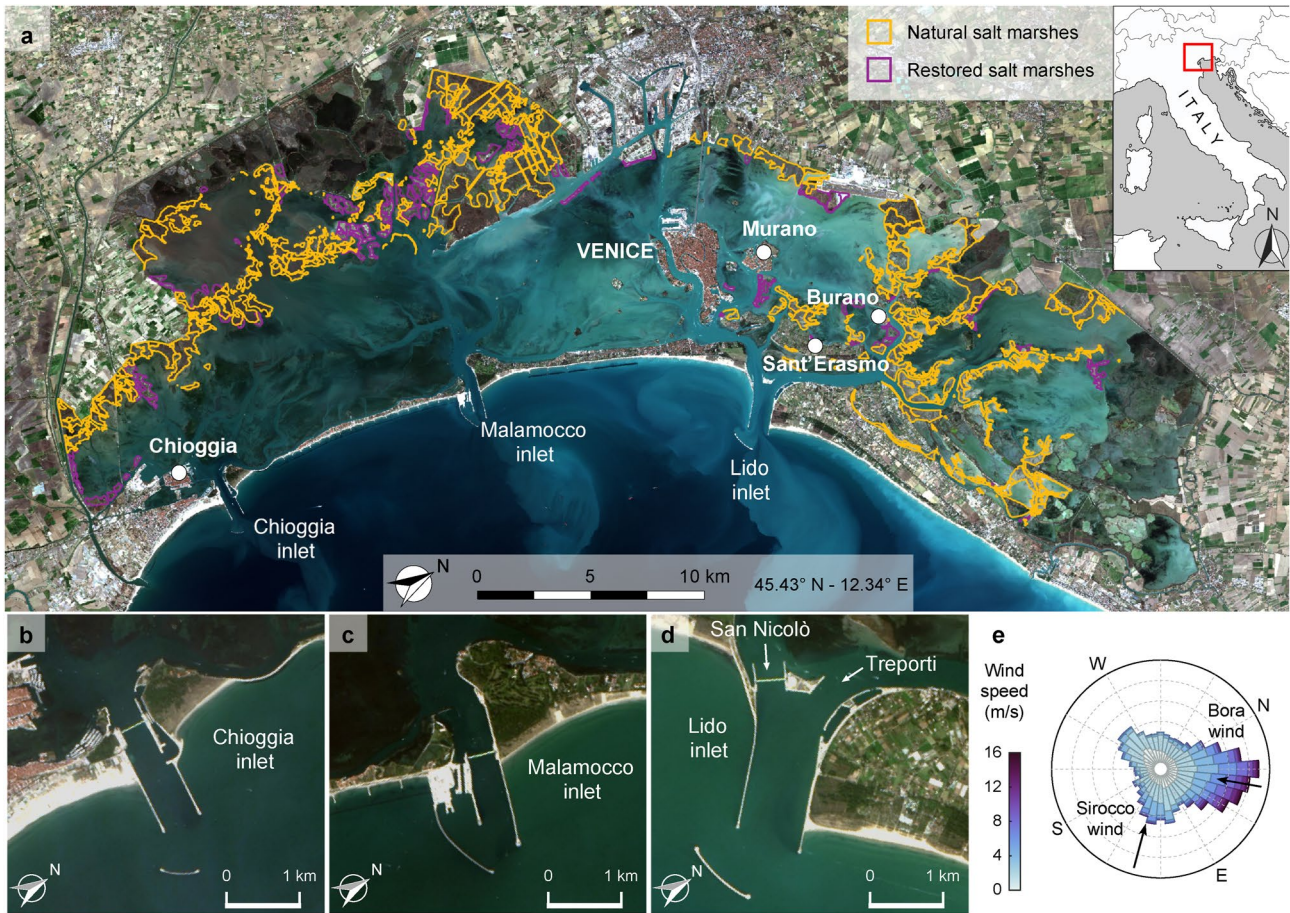


Figure 1. Geomorphological setting. (a) Satellite images of the Venice Lagoon (image Copernicus Sentinel, 2020). Natural salt marshes are bordered in yellow, while restored salt marshes are shown in purple. (b, c, d) Close-up views of the three lagoon inlets. (e) Rose-diagram representation of wind climate recorded at the “Chioggia Diga Sud” anemometric station during the period 2000–2019. The two most relevant winds, that is, the north-easterly *Bora* wind and the south-easterly *Sirocco* wind, are also highlighted.

the design phase (Figures 2a–2c). On the other hand, they caused critical changes in the lagoon hydro- and morpho-dynamic regimes. Since the construction of the jetties, changes in the tidal regime within the lagoon have been much more sustained than the typical periodic, multi-annual variations induced by the nodal modulation of tides in the Adriatic Sea, which are in the order of 4% of the characteristic tidal range (Amos et al., 2010; Valle-Levinson et al., 2021). Between 1909 and 1973, the tidal range within the lagoon increased as much as 25% on average (L. D’Alpaos, 2010; Ferrarin et al., 2015; Tomasin, 1974), with local changes that can be even more pronounced (Finotello, Capperucci, et al., 2022; Finotello et al., 2019; Silvestri et al., 2018).

Changes in the lagoon hydrodynamics due to the construction of the jetties, coupled with eustatic sea-level rise (average value 1.23 ± 0.13 mm/year between 1872 and 2019; 2.76 ± 1.75 mm/year between 1993 and 2019; see Zanchettin et al., 2021), critically impacted on the lagoon morphological evolution, triggering positive morpho-dynamic feedbacks. Progressively larger portions of the lagoon became ebb-dominated, especially close to the inlets where the jetties produced strong flow asymmetries. Asymmetric tidal flows enhanced the export of fine sediments and prevented the import of sediment carried in suspension by longshore currents (L. D’Alpaos, 2010). This condition, worsened by anthropogenically-induced starvation of fluvial sediments, set a negative sediment budget and resulted in a generalized loss of salt marshes (Carniello et al., 2009; L. D’Alpaos, 2010; Tommasini et al., 2019; see Figures 2a–2f and 2k). Reduced marsh coverage lengthened wind fetches, thus favoring the formation of higher, more energetic waves, which further enhanced lateral marsh retreat and prompted erosion of tidal mudflats (Carniello et al., 2009; Finotello et al., 2020; Leonardi, Ganju, & Fagherazzi, 2016; Marani, D’Alpaos et al., 2011; Mariotti & Fagherazzi, 2013; Tommasini et al., 2019; see Figure 2). Mudflat deepening (Figure 2l), exacerbated by eustatic sea-level rise and both natural and anthropogenic-induced subsidence,

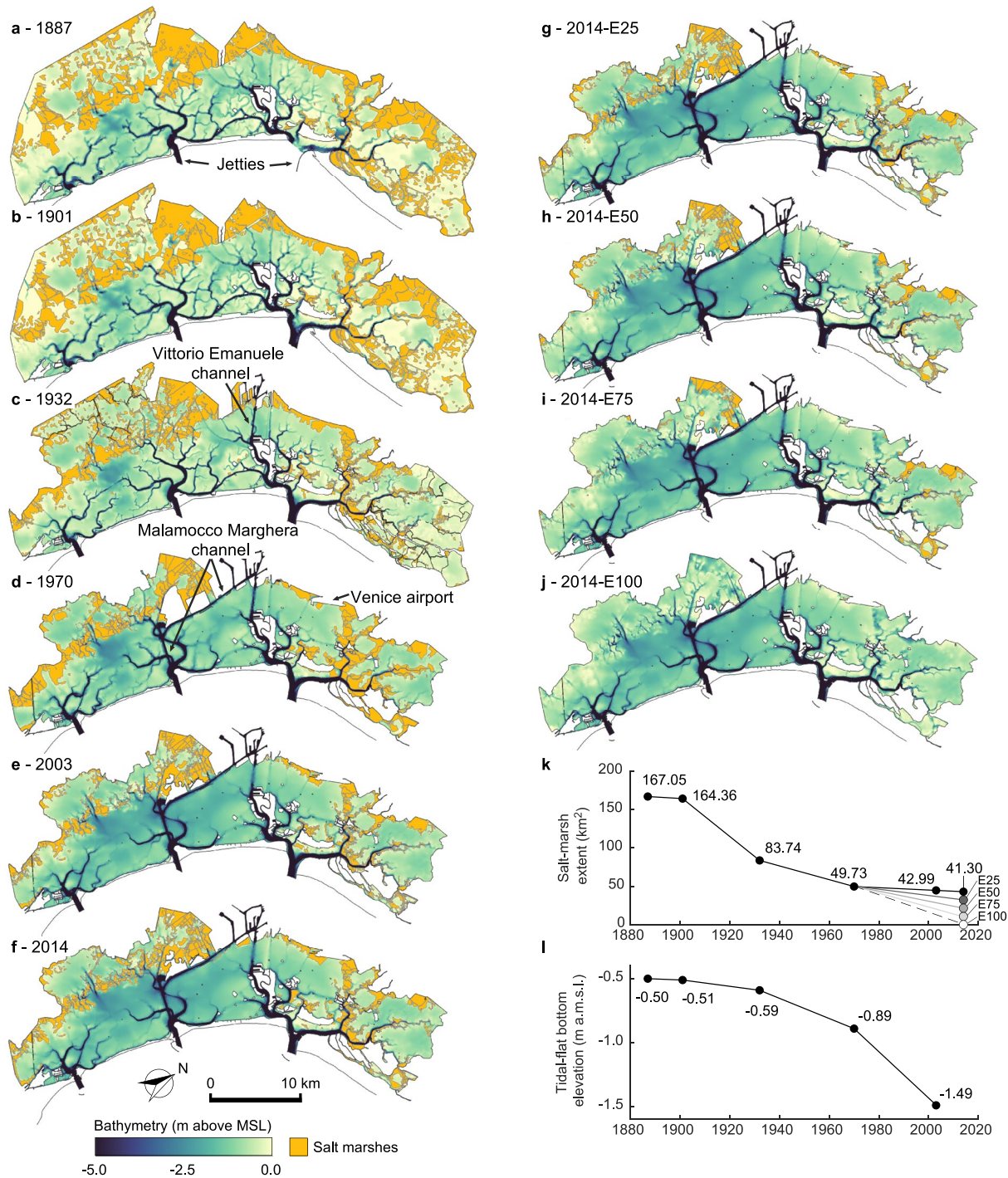


Figure 2. Morphological evolution of the Venice Lagoon. Bathymetry of the Venice Lagoon in 1887 (a), 1901 (b), 1932 (c), 1970 (d), 2003 (e), and 2014 (f), as reconstructed from available historical topographic and bathymetric data. (g, h, i, j) Morphology of the Venice Lagoon according to the hypothetical scenarios of marsh erosion analyzed in the present study. These scenarios assume different rates of marsh erosion equal to 25% (2014-E25), 50% (2014-E50), 75% (2014-E75), and 100% (2014-E100), respectively. Temporal variation of salt-marsh extent (k) and spatially-averaged bottom elevation of tidal flats (l) between 1887 and 2014 are also shown.

promoted the formation of even higher wind waves, which in turn favored additional erosion of salt marshes and mudflats through a positive feedback loop.

Further manmade modifications of the inlet morphologies were carried out between 2006 and 2014 to accommodate the mobile floodgates of the Mo.S.E. (acronym for “Modulo Sperimentale Elettromeccanico”, Electromechanical

Experimental Module) system (Figures 1b–1d), designed to protect the city of Venice and other lagoon settlements from extensive floodings (Mel, Viero, et al., 2021). These interventions slightly increased hydraulic resistances at the inlets and led to both a reduction of tidal amplitudes and an increase in tidal-phase delays within the lagoon (Ghezzi et al., 2010; Matticchio et al., 2017). Salt-marsh erosion is still ongoing nowadays, though at much lower rates compared to the last century (Figure 2k). This is due to a series of critical interventions, aimed at safeguarding and restoring salt marshes, that have been put in place by the Venice Water Authority since the early 1990s, with additional more recent contributions by some EU-funded LIFE projects (Barausse et al., 2015; Tagliapietra et al., 2018; Tommasini et al., 2019; see also www.lifevimine.eu/ and www.lifelagoonrefresh.eu/). At present, about 12% of the existing salt marshes are either entirely artificial or at least partially restored (see purple lines in Figure 1a), and a good portion of the remaining natural ones are protected against lateral erosion by manmade wood piling or berms (see Figure S2 in Supporting Information S1). Clearly, without these restoration and conservation efforts, the total area of salt marshes would be significantly smaller than it currently is.

Finally, it is worthwhile noting that operations of the Mo.S.E. floodgates will further reduce the resilience of salt marshes to rising relative sea levels by reducing inorganic deposition during storm-surge events which, though episodic, critically contribute to marsh vertical accretion (Tognin et al., 2021, 2022).

3. Methods

3.1. Numerical Model

We employed the bidimensional, depth-averaged, finite element numerical model developed by Carniello et al. (2005, 2011), which is suitable to reproduce the hydrodynamics of shallow tidal basins driven by tidal flows and wind fields. In the following, we report a brief description of the model and refer the reader to Carniello et al. (2005, 2011) for further details. The model consists of two coupled modules, namely a hydrodynamic and a wind-wave module, and will be referred to as WWTM (Wind-Wave Tidal Model) hereinafter.

The hydrodynamic model solves a suitably-modified version of the shallow water equations (Defina, 2000) to account for wetting and drying processes in very shallow and irregular domains:

$$\begin{aligned} \frac{\partial q_x}{\partial t} + \frac{\partial}{\partial x} \left(\frac{q_x^2}{Y} \right) + \frac{\partial}{\partial y} \left(\frac{q_x q_y}{Y} \right) - \left(\frac{\partial R_{xx}}{\partial x} + \frac{\partial R_{xy}}{\partial y} \right) + \frac{\tau_{bx}}{\rho} - \frac{\tau_{wx}}{\rho} + gY \frac{\partial H}{\partial x} &= 0 \\ \frac{\partial q_y}{\partial t} + \frac{\partial}{\partial x} \left(\frac{q_x q_y}{Y} \right) + \frac{\partial}{\partial y} \left(\frac{q_y^2}{Y} \right) - \left(\frac{\partial R_{xy}}{\partial x} + \frac{\partial R_{yy}}{\partial y} \right) + \frac{\tau_{by}}{\rho} - \frac{\tau_{wy}}{\rho} + gY \frac{\partial H}{\partial y} &= 0 \\ \eta \frac{\partial H}{\partial t} + \frac{\partial q_x}{\partial x} + \frac{\partial q_y}{\partial y} &= 0 \end{aligned}$$

where t is time, the x and y subscripts denote the directions of a given variable in a Cartesian reference system, q is the flow rate per unit width, R represents the depth-averaged Reynolds stresses, τ_b is the bottom shear stress produced by tidal currents, τ_w is the wind-induced shear stress at the free surface whose elevation is H , ρ stands for water density, g is the gravitational acceleration, Y is the water volume per unit area ponding the bottom (i.e., the equivalent water depth) and η is the wet fraction of the computational domain which accounts for surface irregularities during the wetting and drying processes (see Defina, 2000, for a detailed description of the hydrodynamic equations).

The hydrodynamic module provides the wind-wave module with water levels and depth-averaged velocities that are employed for calculating wave group celerity and bottom shear stresses (induced by both wind waves and tidal currents), as well as for evaluating the influence of flow depth on wind-wave propagation.

The wind-wave module employs the same computational grid of the hydrodynamic model to solve the wave action conservation equation (Holthuijsen et al., 1989). The latter is simplified by assuming that the direction of wave propagation instantaneously readjusts to match the wind direction (i.e., neglecting refraction). The module describes the evolution of the wave action density (N_0) in the frequency domain, which reads (Carniello et al., 2011):

$$\frac{\partial N_0}{\partial t} + \frac{\partial}{\partial x} c'_{gx} N_0 + \frac{\partial}{\partial y} c'_{gy} N_0 = S_0$$

where c'_{gx} and c'_{gy} represent the wave group celerity in the x and y direction, respectively, and are used to approximate the propagation speed of N_0 (Carniello et al., 2005; Holthuijsen et al., 1989), while S_0 represents all the source terms describing the external phenomena contributing to wave energy variations, which can be either positive (wind energy input) or negative (bottom friction, white capping, and depth-induced breaking). Based on the relationship between the peak wave period and local wind speed and water depth (Young & Verhagen, 1996), the model can compute both the spatial and temporal distribution of the wave period. Linear wave theory also allows one to relate the local significant wave height to wind-wave-induced bottom shear stresses (τ_{ww}). The nonlinear interactions between τ_{ww} and current-induced bottom shear stresses (τ_b) are accounted for through the empirical Soulsby's (1995) formulation, which enhances the value of the total bottom shear stress (τ_{wc}) beyond the mere sum of τ_b and τ_{ww} (see details in Carniello et al., 2005, their equations (26) and (27)).

3.2. Numerical Simulations

3.2.1. Computational Grids

Numerical simulations were performed considering 10 different morphological configurations of the Venice Lagoon (Figure 2). Six of these configurations represent past-lagoon morphologies reconstructed from available topographic and bathymetric data (Figures 2a–2f), whereas the additional four configurations consist of hypothetical scenarios characterized by additional marsh loss relative to the present-day lagoon morphology (Figures 2g–2j). Specifically, to understand how marsh loss affected the hydrodynamics of the Venice Lagoon in the past, we utilized six already existing WWTM computational grids representing the morphological configurations of the lagoon from 1887 to 2014 (Figure 2). Each grid faithfully reproduces the lagoon morphological features at the time of the selected topobathymetric surveys (see Figure S3 in Supporting Information S1). The 1887 and 1901 grids were constructed based on “Topographic/hydrographic map of the Venice Lagoon” produced by the Genio Civile of Venezia in 1901, and are identical to each other except for the different morphology of the Lido inlet, where only the northern jetty was present in 1887 while both the jetties were completed in 1901. In contrast, different topographic surveys carried out in 1932, 1970, and 2003 by the Venice Water Authority (Magistrato alle Acque di Venezia) were employed to create the computational grids relative to the years 1932, 1970, 2003, and 2014, respectively (Carniello et al., 2009) (Figures 2a–2e). The 2014 computational grid is based on the most recent, 2003, bathymetric survey and accounts also for the anthropogenic modifications at the three inlets related to the Mo.S.E. system, which were completed in 2014 (Figure 2f). The interested reader is referred to Carniello et al. (2005, 2011) and Tognin et al. (2022) for extensive details regarding the calibration of both the hydrodynamic and the wind-wave model with applications to the Venice Lagoon. Calibration and testing of the model obviously refer to the most recent configurations of the lagoon, for which field data are available. In contrast, local values of the bed-friction coefficient for the older configurations of the lagoon (1932, 1901, 1887) were assumed in analogy with those selected for the calibrated grids, that is, as a function of local sediment grainsize, bed elevation, and the possible presence of vegetation (e.g., in salt marshes). For the sake of brevity, we will report here only a summary of the model performances quantified through the standard Nash-Sutcliffe Model Efficiency (NSE) parameter derived from previous applications of the model, for which measured field data were available in terms of tidal levels and significant wave heights within the Lagoon, as well as flow rates at the lagoon inlets (Carniello et al., 2005, 2011; Tognin et al., 2022). Following the categorization of model performance proposed by Allen et al. (2007), who considered four categories from excellent to poor (i.e., $NSE > 0.65$ excellent; $0.5 < NSE \leq 0.65$ very good; $0.2 < NSE \leq 0.5$ good; $NSE \leq 0.2$ poor), our WWTM model is excellent in reproducing tidal levels ($NSE_{\text{mean}} = 0.970$, $NSE_{\text{median}} = 0.984$, $NSE_{\text{std}} = 0.040$), very good to excellent in reproducing significant wave heights ($NSE_{\text{mean}} = 0.627$, $NSE_{\text{median}} = 0.756$, $NSE_{\text{std}} = 0.357$), and excellent in replicating flow rates at the inlets ($NSE_{\text{mean}} = 0.853$, $NSE_{\text{median}} = 0.931$, $NSE_{\text{std}} = 0.184$). All the statistics were derived based on data reported in Tognin et al. (2022; their Table S2 in Supporting Information S1), as well as in Carniello et al. (2011, their Tables 1, 2, and 3).

In addition to the above, we also investigated the hydrodynamic effects of additional marsh losses based on four possible scenarios characterized by different degrees of wind-wave-driven salt-marsh lateral erosion. These scenarios should be properly interpreted as hypothetical configurations that the present-day lagoon might have assumed if marsh erosion had been more intense and/or if—more realistically—the interventions aimed at safeguarding and restoring salt marshes had not been put in place (Barausse et al., 2015; Tagliapietra et al., 2018; see Figure S2 in Supporting Information S1). Thus, our analysis investigates what the effects of not protecting

and restoring the salt marshes might have been, and somehow provides a baseline for assessing whether or not it is worthwhile to continue such conservation efforts. In the four analyzed scenarios, we accounted for an overall marsh-area loss equal to 25% (E25, Figure 2g), 50% (E50, Figure 2h), 75% (E75, Figure 2i), and 100% (E100, Figure 2j) relative to the present-day marsh extent. The computational grids for each of these four scenarios were constructed utilizing the 2014 computational grid as a baseline, and gradually removing marsh areas following an approach similar to that proposed by Donatelli et al. (2018). Specifically, computational elements located along eroding marsh margins were selected and their characteristics in terms of elevation and roughness were modified to match those of the surrounding tidal flats. Differently from Donatelli et al. (2018) though, the erosion of salt marshes was not spatially uniform, but rather occurred proportionally to the local mean power of wind waves striking the marsh edge (Figure S4 in Supporting Information S1). Since previous studies have demonstrated a linear functional dependence between marsh lateral retreat and the power of incoming waves (Leonardi, Ganju, & Fagherazzi, 2016; Marani, D'alpaos et al., 2011; Mel et al., 2022), cell conversion from salt marsh to mudflat was imposed proportionally to the value of local wind-wave power derived from literature data (Figure S4 in Supporting Information S1; Finotello et al., 2020; Tommasini et al., 2019).

Although salt-marsh loss alters the water volume exchanged between the sea and the lagoon (i.e., tidal prism) and the inlet cross-sectional area should adjust consequently according to the O'Brien-Jarret-Marchi law (A. D'Alpaos et al., 2009; Jarrett, 1976), in the hypothetical scenarios involving additional marsh erosion the geometry of the lagoon inlets was kept unaltered compared to the present-day configuration. This is because the current geometry of the inlets is fixed both horizontally and vertically by the presence of the jetties and the concrete housing structures built to host the Mo.S.E. floodgates. Besides, the scour processes induced by the jetties during the last century deepened the inlets down to the overconsolidated *Caranto* layer, which would have prevented any further deepening even if the Mo.S.E. barriers had not been constructed.

3.2.2. Boundary Conditions

In the numerical model, water levels are imposed at the seaward boundary of the computational domain representing the portion of the northern Adriatic Sea in front of the Venice Lagoon (see Figure 3b). Water-level data are measured at the CNR Oceanographic Platform, which is located in the Adriatic Sea approximately 15 km away from the coastline. Because water levels and bed elevations in each computational grid refer to the mean sea level at the time of each survey, historical rises in relative sea level are implicitly accounted for. Wind speeds and directions are measured at the "Chioggia Diga Sud" anemometric station (Figure 3b) and applied to the whole lagoonal basin (see Carniello et al., 2005 for details).

All the simulations were carried out employing the same boundary conditions, thus allowing for direct comparisons between different lagoon configurations. Specifically, the model was forced using hourly water levels and both wind velocities and directions measured from 16 November 2005 to 17 December 2005 (Figure 3a). The selected 30-day period is representative of hydro-meteorological conditions experienced every year by the Venice Lagoon between October 1st and January 30th, which is the period typically characterized by the most significant storm-surge events. More in detail, the cumulative frequency of water levels for the selected study period is the closest to the average distribution observed between 2000 and 2020 (Figure 3c). Moreover, the study period is characterized by two relatively strong *Bora* wind events (Figure 3a) that are typical of the wind climate observed in Venice (Figure 3d). Thus, the selected study period allows for focusing both on characteristic tides as well as on representative storm events.

4. Results

The hydrodynamic effects of morphological changes at the lagoon scale were investigated by considering different parameters related to both tides and wind waves.

4.1. Water Levels

Concerning water levels, we first focused on the mean tidal range (*MTR*, Figure 4), computed as the average difference between consecutive high- and low-tide water levels. Results show a continued increase of *MTR* from 1887 to 2003, though spatially-explicit representations suggest that this increase is not homogeneous. Increases in *MTR* between 1887 and 1901 are mostly limited to the northern lagoon (Figures 4a and 4b), whereas between 1901 and 1932 enhanced *MTR* values are observed especially in the southern lagoon and in the surroundings of

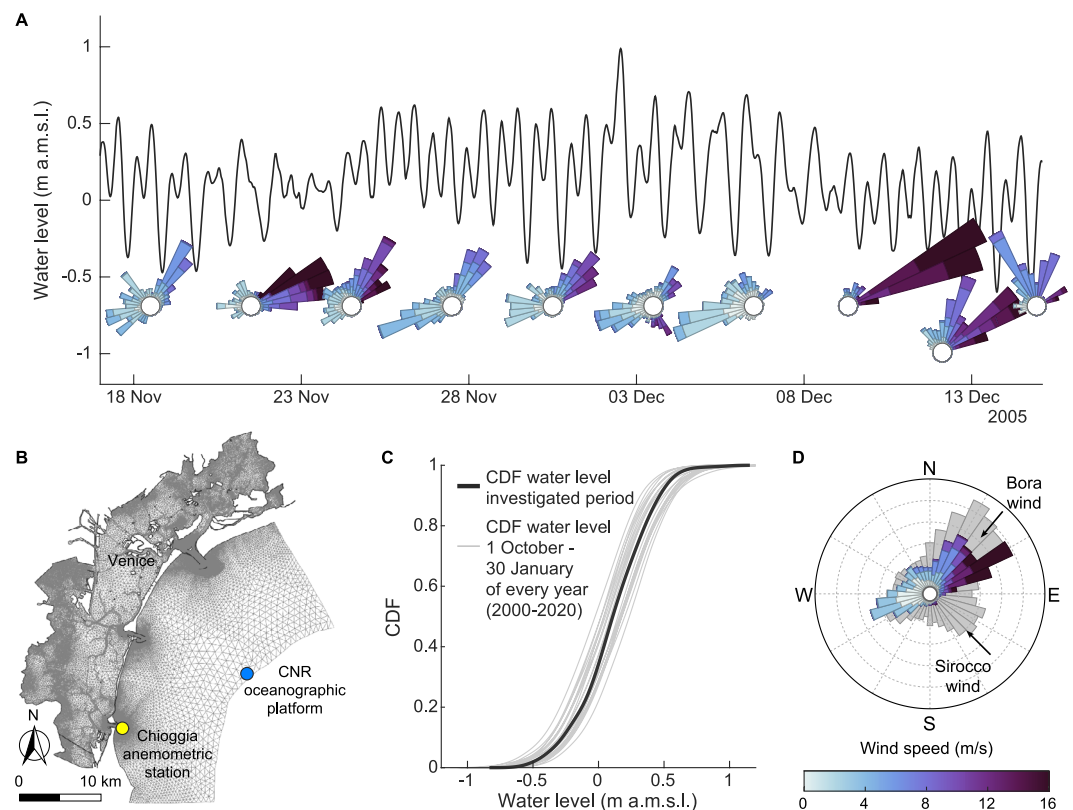


Figure 3. Numerical modeling and boundary conditions. (a) Water level and wind climate data utilized in the numerical simulations. Data refer to the period 17 November 2005–17 December 2005. Water levels were measured at the “CNR Oceanographic Platform”, whereas wind data were retrieved from the “Chioggia Diga Sud” anemometric station (see panel b). (b) An example of the computational grid employed by the numerical model, referred to the 2014 morphological configuration of the Venice Lagoon. (c, d) Distributions of water levels (c) and wind climate (d) during the analyzed period are compared to those observed over the period 2000–2019 (in gray).

Venice City (Figures 4b and 4c). The most pronounced and generalized increase in *MTR* is observed between 1932 and 1970 (Figure 4d), as a result of extensive losses of marshlands, disappearance of minor branches of tidal channel networks, and generalized tidal-flat deepening (Figure 2d). In contrast, only minor changes are observed from 1970 onwards (Figures 4d–4f), with probability distributions suggesting only a slight increase in *MTR* between 1970 and 2003 followed by a reduction between 2003 and 2014 (Figure 4k). Numerical simulations involving additional losses of salt-marsh areas suggest slight reductions in *MTR* proportionally to the percentage of marsh area being lost (Figure 4l).

Since *MTR* does not embed information regarding modifications of high water levels, changes in the Mean High Water Level (*MHWL*) were also assessed. The *MHWL* is defined as the average of all the water level maxima observed during the study period and it thus represents a meaningful proxy to estimate changes in flooding risk in urban areas within the lagoon. Overall, a generalized increase in *MHWL* occurred during the study period (Figures 5a–5f). A slight attenuation of *MHWL* is observed between 1901 and 1932 (Figure 5k), followed by a pronounced increase between 1932 and 1970 (Figure 5k), when more than half of the total marsh area was already lost (Figure 2k) and the lagoon underwent significant morphological changes (Figures 2c and 2d). After 1970, only minor increases in *MHWL* are observed until 2014 (Figure 5k). Nonetheless, simulations in the hypothetical scenarios suggest that additional losses of salt marshes could have resulted in further *MHWL* increases relative to the values observed in 2014 (Figure 5).

4.2. Wind Waves and Bottom Shear Stresses

Wind waves play a fundamental role in the hydrodynamics and morphodynamics of shallow tidal systems, in general (e.g., Green & Coco, 2014), and of the Venice Lagoon, in particular (Carniello et al., 2009, 2011, 2012).

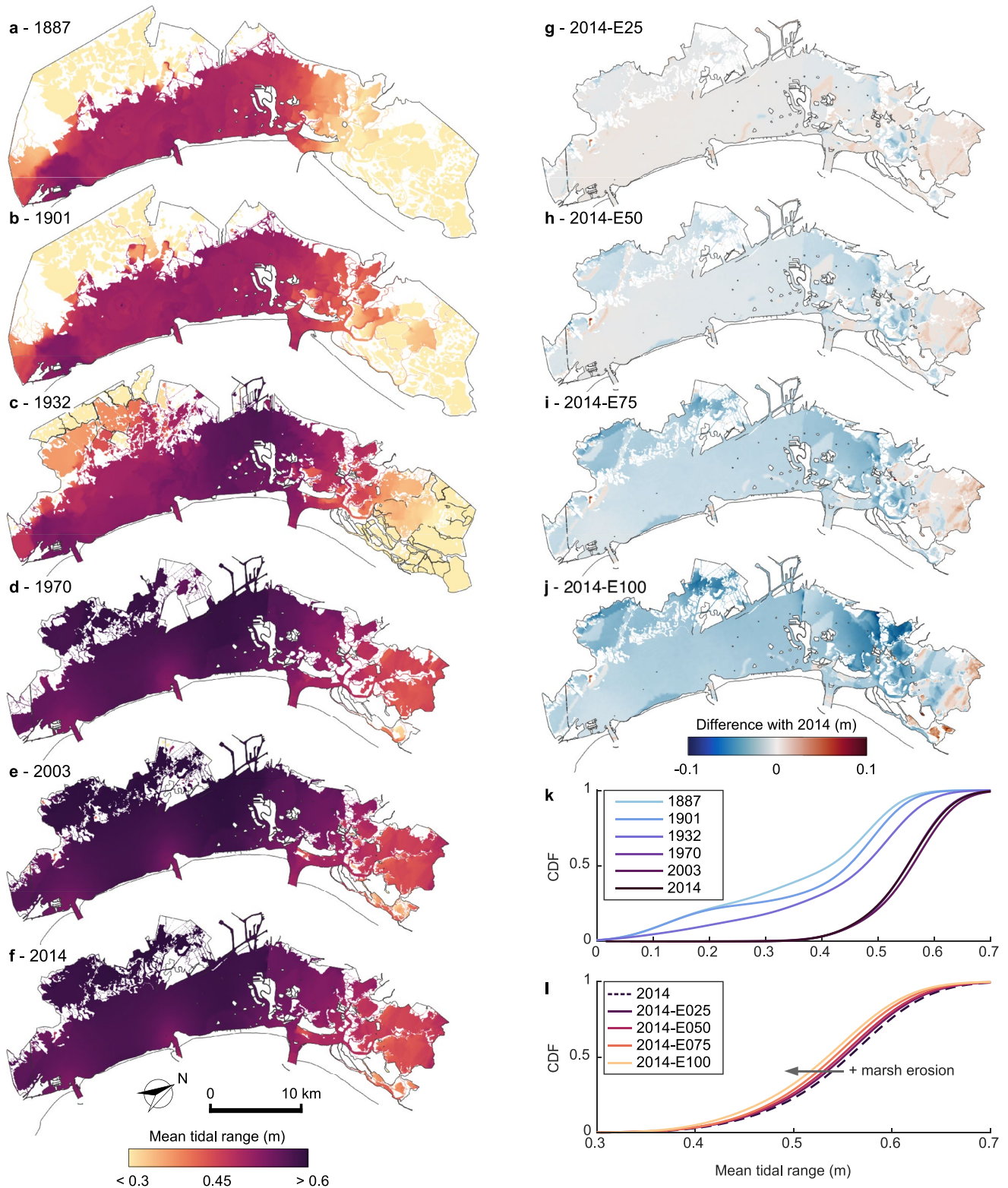


Figure 4. Evolution of mean tidal range (*MTR*). Spatially-explicit representation of *MTR* in 1887 (a), 1901 (b), 1932 (c), 1970 (d), 2003 (e), 2014 (f). Difference between the 2014 configuration and the hypothetical marsh-erosion scenarios: 2014-E25 (g), 2014-E50 (h), 2014-E75 (i), 2014-E100 (j). (k) Cumulative frequency (CDF) of *MTR* for the historical configurations (1887–2014). (l) Cumulative frequency of *MTR* in the hypothetical marsh erosion scenarios (2014-E25, E50, E75, E100).

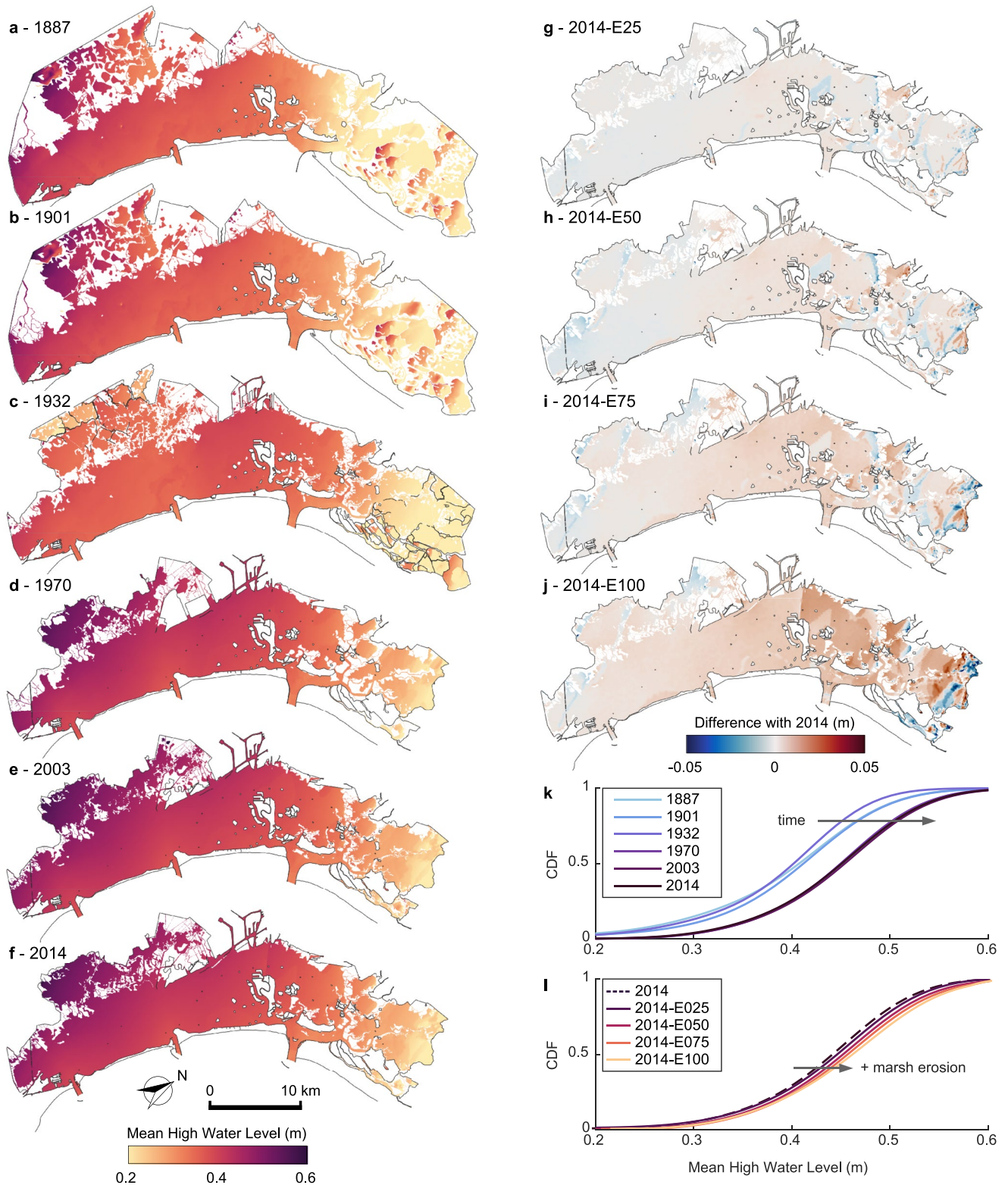


Figure 5. Evolution of mean-high water level (*MHWL*). Spatially-explicit representation of *MHWL* in 1887 (a), 1901 (b), 1932 (c), 1970 (d), 2003 (e), 2014 (f). Difference between the 2014 configuration and the hypothetical marsh-erosion scenarios: 2014-E25 (g), 2014-E50 (h), 2014-E75 (i), 2014-E100 (j). (k) Cumulative frequency (CDF) of *MHWL* for the historical configurations (1887–2014). (l) Cumulative frequency of *MHWL* in the hypothetical marsh erosion scenarios (2014-E25, E50, E75, E100).

Here we focus on change in the maximum significant wave height (H_{sMAX} , Figure 6). H_{sMAX} invariably increases through time in all the considered historical configurations, but only minor changes occurred before 1932 (Figures 6a–6c,k). In contrast, between 1932 and 1970, pronounced increases in H_{sMAX} are observed, especially in the central and southern portions of the lagoon that are more exposed to the action of *Bora* winds (Figure 6d). Although after 1970 the distribution of H_{sMAX} does not display substantial changes (Figure 6e,f,k), numerical simulations considering additional losses of salt marshes suggest that H_{sMAX} would have further increased proportionally to the percentage of marsh area being lost (Figures 6g–6j and 6l). The most important increases in H_{sMAX} would have occurred in areas that are presently occupied by extensive salt marshes (Figures 6g–6j), that is, the whole northern lagoon as well as the most landward portions of the central-southern lagoon (see Figure 2f).

The key role exerted by wind waves on the lagoon morphodynamics is related to their ability to determine sediment resuspension from shallow tidal-flat areas, a process whose intensity depends nonlinearly on wave characteristics. Wind waves produce bottom shear stresses (τ_{ww}) that compound the bottom shear stresses induced by tidal currents (τ_b) and determine the total shear stresses (τ_{wc}) that eventually lead to sediment resuspension when τ_{wc} exceeds the critical threshold for erosion (Carniello et al., 2012; see Section 3.1). Numerical results suggest that within tidal channels, where τ_b is typically dominant, only minor increases in τ_{wc} maxima occurred over time (Figures 7a–7f). In contrast, across shallow mudflats where the wave-induced bottom shear stress component (τ_{ww}) is predominant, the maximum values of τ_{wc} invariably increased from 1887 to 2014 (Figures 7a–7f). This is consistent with changes in maximum wave heights (H_{sMAX}), and results in a generalized increase of τ_{wc} across the entire lagoon that is especially clear between 1932 and 1970 (Figure 7k). Numerical simulations with additional losses of salt marshes suggest that τ_{wc} maxima would have been further enhanced proportionally to the marsh area being lost (Figures 7g–7j, 7l).

4.3. Tidal Asymmetries

Larger values of bottom shear stress increase the chance for sediments to be resuspended and transported elsewhere by tides and wave-induced currents, thus affecting the overall lagoon sediment budget. In particular, previous studies showed that asymmetries in tidal currents (Aubrey & Speer, 1985; Murty, 1990) are critical in determining the ultimate fate of sediments carried in suspension, with ebb-dominated tidal flow leading to sediment export to the open sea and, therefore, to a net erosion of the lagoon. Here we quantified tidal asymmetries (γ) using the formulation proposed by Nidzicko (2010). This formulation allows for a spatially-explicit computation of γ based on the normalized skewness of the water level time derivative ($\partial\zeta/\partial t = \zeta'$):

$$\gamma = \frac{\mu_3}{\sigma^3} = \frac{\frac{1}{T-1} \sum_{t=1}^T (\zeta'_t - \bar{\zeta}')^3}{\left[\frac{1}{T-1} \sum_{t=1}^T (\zeta'_t - \bar{\zeta}')^2 \right]^{3/2}}$$

where μ_3 is the third sample moment about the mean, σ is the standard deviation, and T is the sampling timeframe. Negative values of γ indicate ebb dominance, whereas flood-dominated tides are characterized by positive values of γ . Our results suggest that progressively larger portions of the Venice Lagoon became ebb-dominated over time (Figures 8a–8f). Pronounced changes in tidal asymmetry in the surroundings of the Lido inlet can be observed between 1887 and 1901 (Figure 8b), immediately after the construction of the jetties. Similarly, an extensive expansion of the areas dominated by ebb tides is highlighted after the construction of the jetties at the Chioggia inlet in 1932 (Figure 8c). Afterwards, the hydrodynamic regime of many portions of the lagoon shifted from flood- to ebb-dominated, especially close to the Malamocco inlet where the Malamocco-Marghera canal was excavated (Figures 8d–8f). The most pronounced changes in the hydrodynamic regime of the lagoon occurred between 1932 and 1970 (Figure 8k), when most of the salt marshes had already been lost and the deepening rate of tidal flats accelerated (see Figure 2k–2l). Numerical simulations demonstrate that the effects of additional marsh losses on γ would have not been negligible (Figures 8g–8j). Overall, ebb dominance is slightly reduced as salt marshes are progressively eroded (Figure 8l), but distinct trends of γ changes are observed as a function of the distance from the lagoon inlets. Specifically, while ebb dominance is either maintained or enhanced in the portions of the lagoon proximal to the inlets, a shift to flood dominance is observed in most distal regions where extensive salt marshes are still found nowadays (Figures 8g–8j).

5. Discussion

Our analyses highlight the difficult task of unravelling the hydrodynamic consequences of salt-marsh loss in shallow back-barrier systems. Conceptualized scenarios that assume additional marsh losses without any further

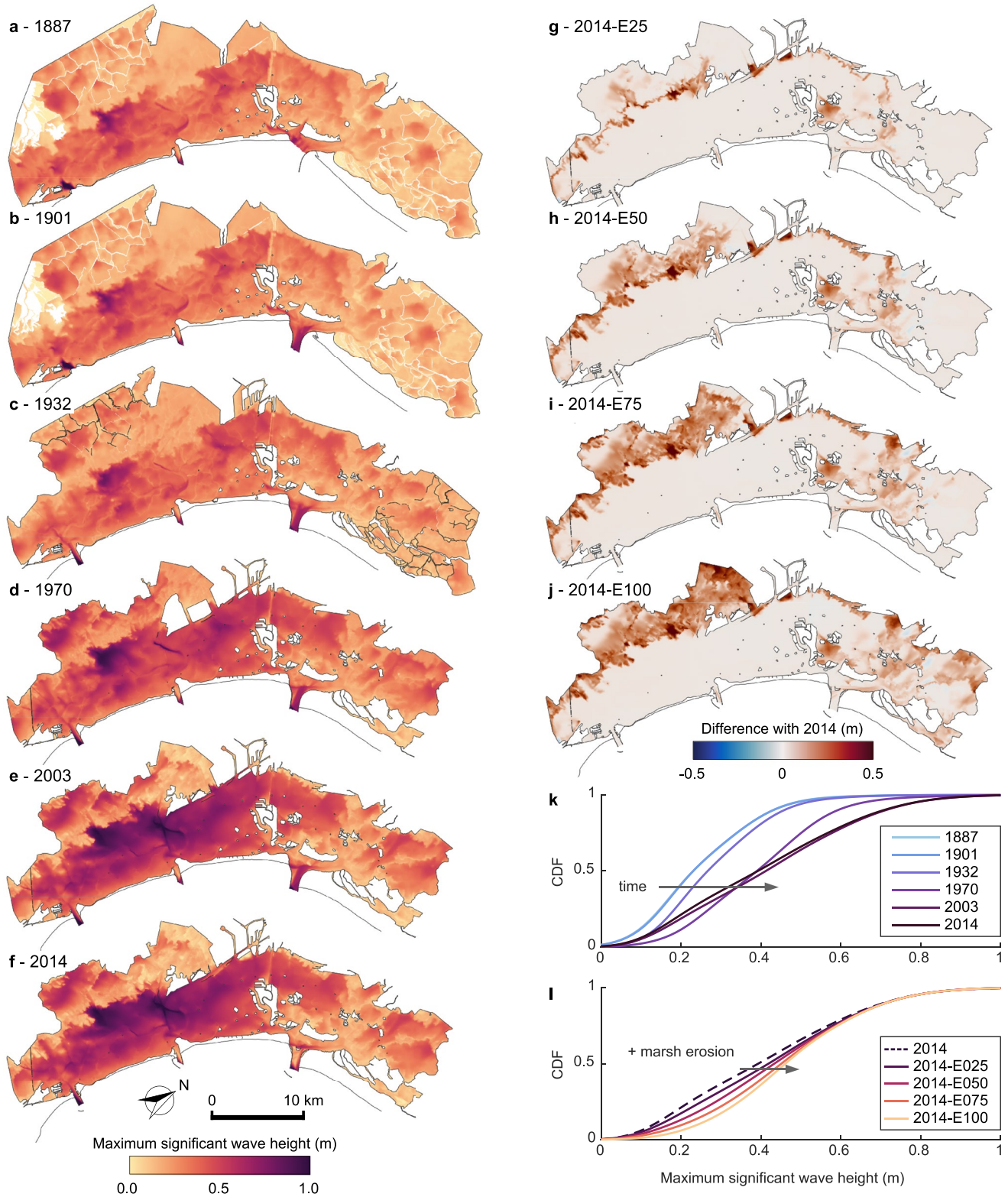


Figure 6. Evolution of maximum significant wave height ($H_{s,max}$). Spatially-explicit representation of $H_{s,max}$ in 1887 (a), 1901 (b), 1932 (c), 1970 (d), 2003 (e), 2014 (f). Difference between the 2014 configuration and the hypothetical marsh-erosion scenarios: 2014-E25 (g), 2014-E50 (h), 2014-E75 (i), 2014-E100 (j). (k) Cumulative frequency (CDF) of $H_{s,max}$ for the historical configurations (1887–2014). (l) Cumulative frequency of $H_{s,max}$ in the hypothetical marsh erosion scenarios (2014-E25, E50, E75, E100).

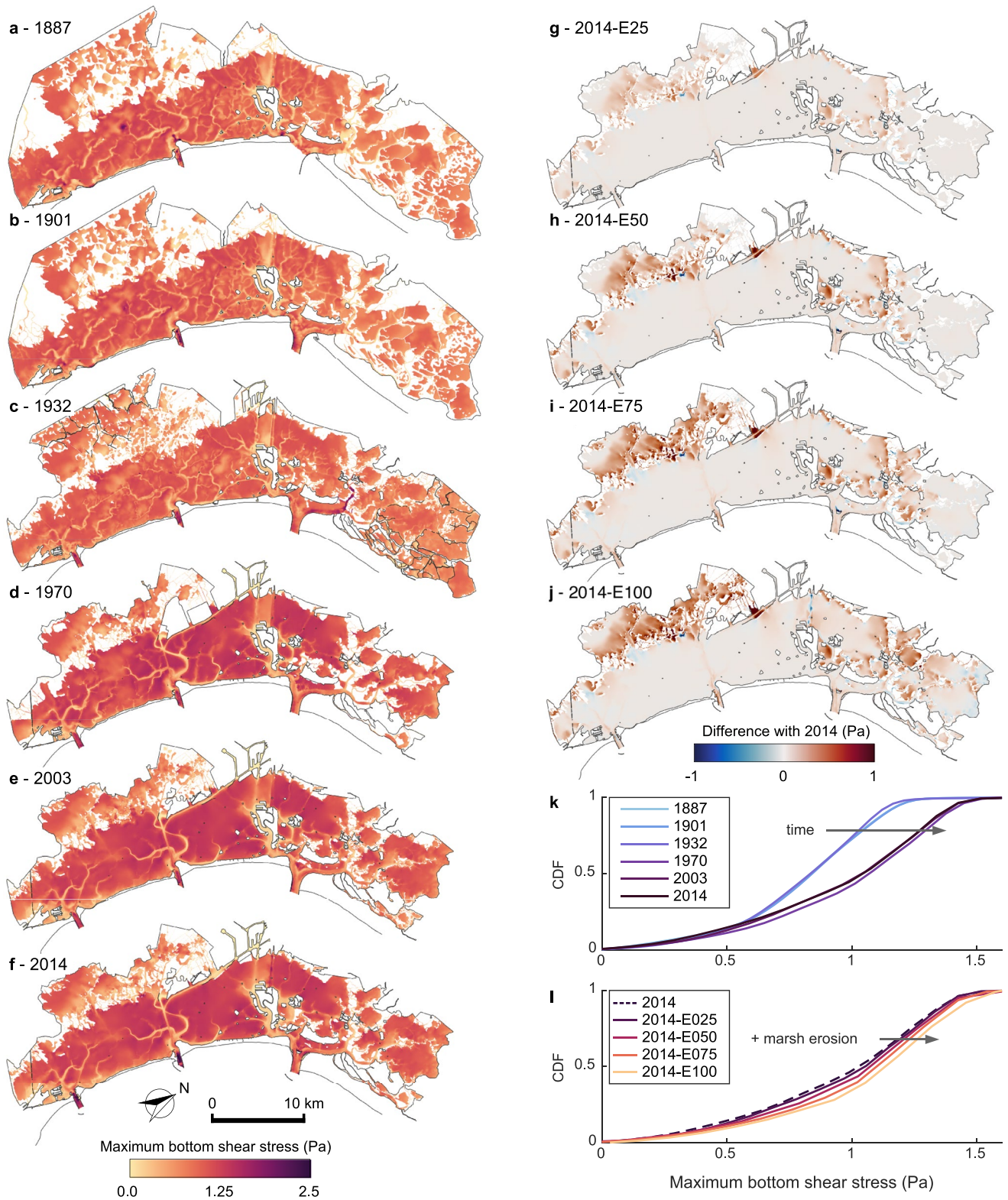


Figure 7. Evolution of maximum bottom shear stress (τ_{wc}). Spatially-explicit representation of τ_{wc} in 1887 (a), 1901 (b), 1932 (c), 1970 (d), 2003 (e), 2014 (f). Difference between the 2014 configuration and the hypothetical marsh-erosion scenarios: 2014-E25 (g), 2014-E50 (h), 2014-E75 (i), 2014-E100 (j). (k) Cumulative frequency (CDF) of τ_{wc} for the historical configurations (1887–2014). (l) Cumulative frequency of τ_{wc} in the hypothetical marsh erosion scenarios (2014-E25, E50, E75, E100).

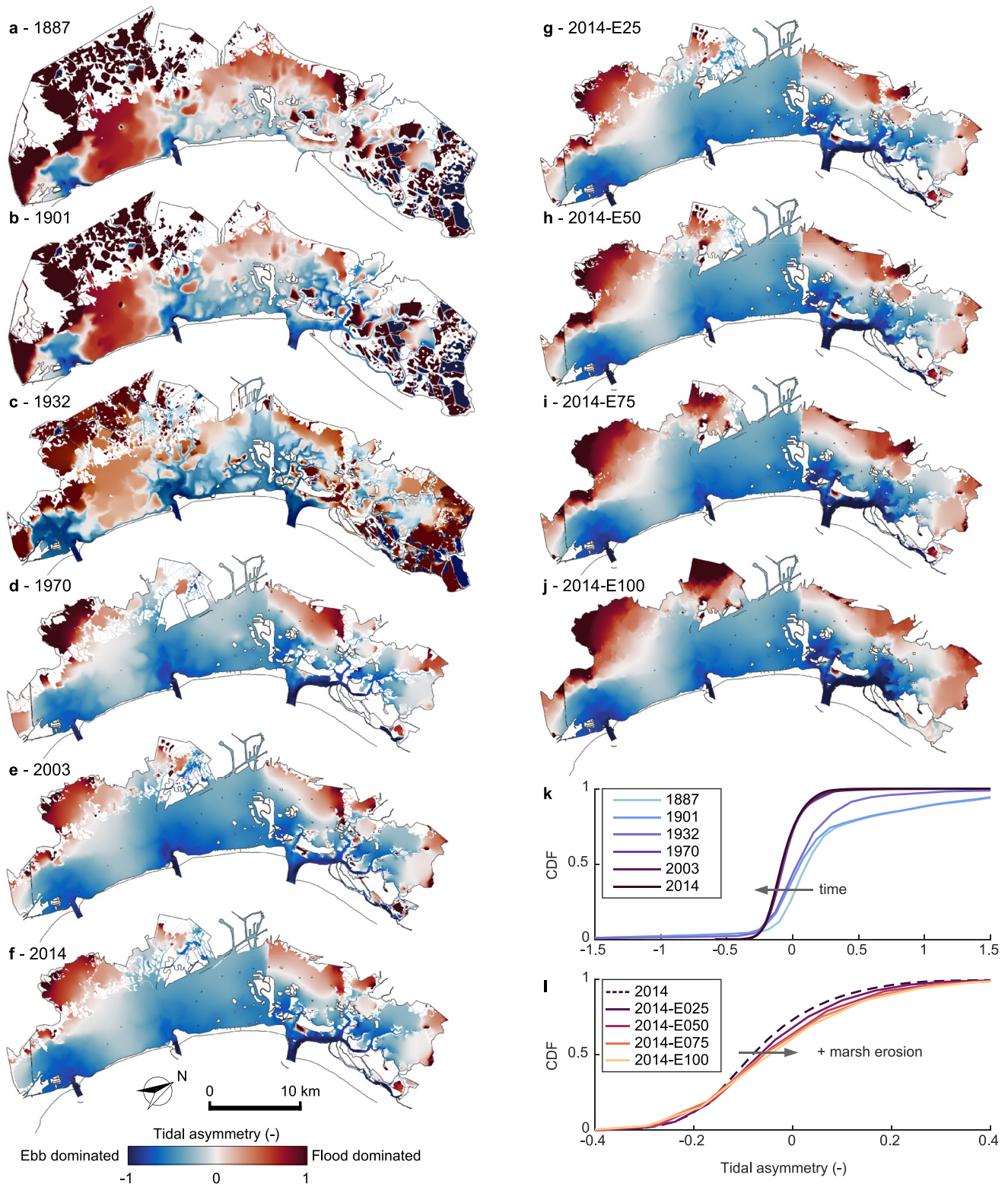


Figure 8. Evolution of tidal asymmetry (γ). Spatially-explicit representation of γ in 1887 (a), 1901 (b), 1932 (c), 1970 (d), 2003 (e), 2014 (f), 2014-E25 (g), 2014-E50 (h), 2014-E75 (i), 2014-E100 (j). (k) Cumulative frequency (CDF) of γ for the historical configurations (1887–2014). (l) Cumulative frequency of γ in the hypothetical marsh erosion scenarios (2014-E25, E50, E75, E100).

modification of the lagoon morphology help to isolate the direct effects of marsh disappearance on the lagoon hydrodynamics. In contrast, indirect, cascade effects due to morphodynamics feedbacks are more easily understood based on numerical results obtained for the historical configurations of the Venice Lagoon.

5.1. Water Levels

How marsh disappearance affects water levels within the lagoon is perhaps the most controversial point to debate. This is because salt marshes are most effective in regulating water levels in the upper intertidal frame due to their characteristic topographic elevations that exceed the mean sea level. Conversely, at lower water stages, marshes are not typically flooded and thus have limited effects on tide propagation, which takes place predominantly within major tidal channels and across tidal flats.

Our simulations of hypothetical marsh-loss scenarios (E25 to E100 runs, Figure 4l) suggest that marsh erosion overall increases accommodation in the back-barrier system, thus reducing the average amplitude of tidal oscillations and, therefore, the mean tidal range (*MTR*). This is in agreement with the results of the numerical experiments carried out in other back-barrier tidal systems along the continental US coast (e.g., Donatelli et al., 2018). However, our analyses also highlight a continued increase in *MTR* (Figure 4k) during the last century. This is most likely a result of both anthropogenic modifications of the lagoon inlets and reduced bottom friction due to mudflat deepening (e.g., Carniello et al., 2009; D'Alpaos & Martini, 2005; Ferrarin et al., 2015; Tambroni & Seminara, 2006) (Figures 2a–2f). Therefore, enhanced *MTR* is only partially related, both directly and indirectly, to salt-marsh loss. This is supported by the local increase of *MTR* after the construction of jetties at the inlets of Lido (1901, Figure 4b) and Chioggia (1932, Figure 4c). Besides, generalized increases in *MTR* occurred between 1932 and 1970 (Figure 4d) as a consequence of tidal-flat deepening. Excavation of the Vittorio Emanuele and Malamocco-Marghera waterways also likely contributed to enhancing *MTR*, especially in the central part of the lagoon (Figures 4c and 4d). Finally, slight reductions in *MTR* between 2003 and 2014 are related to enhanced hydraulic resistance at the inlets produced by the Mo.S.E. structures (Figure 4k) (Matticchio et al., 2017), and are therefore not directly linked to changes in salt-marsh extent.

Similarly, the continued increase in mean high water levels (*MHWL*) observed since 1887 should be only partially considered as a direct effect of marsh loss (Figures 5a–5f). Our simulations suggest that progressive, additional loss of salt marshes would have resulted in further *MHWL* increases (Figures 5g–5j). This is most probably related to the progressive fading of energy dissipations produced by the presence of marshes at high-water stages. Reduced energy dissipations for high-water levels magnify tidal peaks, thus enhancing *MHWL*. Larger *MHWL* potentially bears negative consequences in terms of increased flooding risk of urban settlements (Ferrighi, 2005; Gambolati & Teatini, 2014; Rinaldo et al., 2008). However, one should appreciate that marsh loss preferentially leads to larger *MHWL* in the innermost portions of the northern and central-southern lagoon where marshes are still widespread nowadays (Figures 5g–5j). Conversely, limited changes in *MHWL* are observed in the proximity of the inlets and around the major urban settlements, namely Venice city, Chioggia, and the islands of Murano, Burano, and Sant'Erasmus. For these locations, changes in *MHWL* are less than 3% even if marshes would entirely disappear (E100 scenario), with even lower variations (<2%) in terms of maximum high-water levels. Hence, the effects of salt-marsh loss on back-barrier hydrodynamics appear to be extremely site-specific, with significant hydrodynamic modifications being observed over distances of a few kilometers even within a given tidal embayment.

5.2. Wind Waves and Bottom Shear Stresses

The direct effects of marsh erosion on significant wave heights (H_{sMAX} , Figure 6) and the associated bottom shear stresses (τ_{wc} , Figure 7) are quite straightforward. Before 1932 the generation and propagation of large wind waves were hampered by widespread salt marshes (Figures 2a–2c) that limited wind fetches, as well as by the reduced mudflat depths, which promoted significant wave-energy dissipation (Figures 6a–6c). From 1970 onwards, in contrast, salt-marsh losses coupled with tidal-flat deepening led to increasing H_{sMAX} (Figures 6d–6f) (Defina et al., 2007; Fagherazzi et al., 2006). Reduced marsh coverage favored larger H_{sMAX} due to longer fetches, as confirmed also by numerical simulations involving additional marsh losses (Figures 6g–6j). The most significant increases in H_{sMAX} would have occurred in areas that are nowadays occupied by extensive salt marshes, that is, the northern lagoon as well as the innermost portions of the central-southern lagoon (see Figure 2f). Here, the

disappearance of salt marshes would have reduced their wind-sheltering effect and lengthened wind fetches, eventually leading to the generation and propagation of higher waves (Figures 6g–6j).

Larger $H_{S\text{MAX}}$ also have negative implications for flooding risk in topographically-depressed urban areas, which may be exacerbated when bank overtopping occurs (Gambolati & Teatini, 2014; Mel, Carniello, & D'Alpaos, 2021; Mel, Viero, et al., 2021; Ruol et al., 2020). Nevertheless, our analyses show that $H_{S\text{MAX}}$ and the associated flooding risk are not likely to increase in the marsh-erosion scenarios near the major urban settlements. Even assuming the total disappearance of salt marshes (E100 scenario), increments lower than 5% in $H_{S\text{MAX}}$ are observed near Venice City and the inhabited centers of Chioggia, Murano, Burano, and Sant'Erasmus. This is because all these locations lie far from extensive salt-marsh areas and are little affected by salt-marsh losses. In contrast, at the landward margins of the lagoon where extensive salt-marsh areas are still found nowadays, additional marsh erosion could have led to a threefold to fourfold increase in $H_{S\text{MAX}}$. Values of $H_{S\text{MAX}} > 60$ cm compared to $H_{S\text{MAX}} = 15\text{--}20$ cm in the pre-erosion condition confirm the ability of salt marshes to dissipate wave energy and reduce flooding risk in the lagoon most marginal areas.

Notably, higher waves are also likely to threaten the conservation of the remaining salt-marsh ecosystems, due to the positive feedback mechanism between marsh lateral erosion and wind-wave power (Carniello et al., 2016; A. D'Alpaos et al., 2013; Finotello et al., 2020; Leonardi, Defne, et al., 2016; Marani, D'Alpaos et al., 2011; Tommasini et al., 2019). Specifically, salt-marsh lateral retreat rates are linearly correlated to wave power (P_w) (Finotello et al., 2020; Leonardi, Ganju, & Fagherazzi, 2016; Marani, D'Alpaos et al., 2011; Tommasini et al., 2019), which in turn is a quadratic function of wave height. Hence, salt-marsh loss leads to higher, more energetic waves, which in turn enhance marsh lateral retreat even further in a superlinear fashion. In addition, higher waves also produce larger bottom shear stresses, especially across extensive tidal-flat areas (Figure 7). Our simulations demonstrate that additional losses of salt marshes would have further enhanced τ_{wc} proportionally to the marsh area being lost (Figures 7g–7j.1). This is because the wind sheltering effect typically offered by marshes would have been progressively reduced, allowing for increasingly higher waves to winnow the lagoon bottom (Carniello et al., 2014, 2016; A. D'Alpaos et al., 2013; Tommasini et al., 2019). From a morphodynamic standpoint, the implications of increasing τ_{wc} can be manifold. Larger τ_{wc} will enhance sediment entrainment from the lagoon shallows, producing higher concentrations of suspended sediment ($S\text{SC}$) (Tognin et al., 2022). Wave-driven resuspension from tidal flats represents a key source of sediment for salt marshes in sediment-starving shallow tidal embayments, where the majority of mineral sediments are delivered to the marsh surface during storm-surge events concomitant with strong wave activity (Tognin et al., 2021). Thus, enhanced $S\text{SC}$ could ensure higher resilience of salt-marsh ecosystems in the face of rising relative sea levels (Elsey-Quirk et al., 2019; Mariotti & Fagherazzi, 2010; Tognin et al., 2021). However, such a beneficial effect is likely offset by marsh loss via lateral retreat, which would reduce the total marsh area and promote fragmentation, in this way hampering marsh ability to capture suspended sediment and cope with sea-level rise (Donatelli, Zhang, et al., 2020; Duran Vinent et al., 2021). Besides, enhanced $S\text{SC}$, coupled with the generally ebb-dominated character of tides (Figure 8 and see Section 5.3), are likely to negatively affect the lagoon net-sediment budget, leading to further tidal flat deepening and salt marsh losses.

5.3. Tidal Asymmetries

Salt-marsh loss affects tidal asymmetry (γ) mostly in an indirect fashion, with manmade modifications on the lagoon inlets playing in contrast a critical role (L. D'Alpaos, 2010; L. D'Alpaos & Martini, 2005; Matticchio et al., 2017; Tambroni & Seminara, 2006). Indeed, ebb dominance was increased after the completion of the jetties both at the Lido (Figure 8b) and Chioggia inlets (Figure 8c). Indirect effects of salt-marsh loss on γ could instead arise from the positive morphodynamic feedback between marsh loss and tidal-flat deepening (Carniello et al., 2008, 2009; Defina et al., 2007). This feedback is likely responsible for the shift from flood- to ebb-dominance observed in many portions of the lagoon between 1932 and 1970, especially in the area facing the Malamocco inlet where the Malamocco-Marghera shipway was excavated (Ferrarin et al., 2015) (Figures 8d and 8e). This speculation is supported by earlier results showing how deeper tidal flats reduce bottom friction and ultimately enhance ebb-dominance (Dronkers, 1986; Fortunato & Oliveira, 2005; Friedrichs, 2012; Guo et al., 2019). Our numerical simulations demonstrate also that the direct effects of additional marsh losses on γ are potentially not negligible, with progressive marsh erosion leading to more widespread flood-dominated areas in the innermost portions of the lagoon (Figures 8g–8j). This result is consistent with evidence from previous studies

showing that decreasing intertidal storage capacity associated with gradual marsh losses would re-establish the flood dominance typically observed for progressive tidal waves (Dronkers, 1986; Rinaldo et al., 1999). Despite increased flood dominance due to the marsh disappearance, the tidal regime in most of the lagoon would have remained ebb-dominated (Figures 8g–8j). Thus, a reversal of the current erosional trend and the establishment of a positive net sediment budget would have been unlikely. However, given the nonlinear dependence of sediment transport processes on both tidal flow velocities and asymmetry, these hypotheses should be verified by ad hoc morphodynamic simulations.

5.4. Implications for the Hydrodynamics of Back-Barrier Tidal Lagoons

Our analyses highlight both direct and indirect effects of salt-marsh deterioration on the hydrodynamics of the Venice Lagoon. Despite being generally consistent with previous studies carried out in different tidal settings (e.g., Donatelli et al., 2018; Donatelli, Kalra, et al., 2020; Donatelli, Zhang, et al., 2020), care should be given to generalizing our results to back-barrier tidal embayments morphologically and hydrodynamically different from the study case at hand. The reasons behind this caution are manifold, though all broadly related to the morphological and hydrodynamic peculiarities that characterize each tidal environment, as well as to the conceptualizations we adopted in our numerical simulations.

First, the hydrodynamic response of a tidal system to marsh erosion depends on (a) the planform geometry and hypsometry of the basin (Deb et al., 2022; Van Maanen et al., 2013); (b) the characteristics of tides, especially in terms of tidal range and progressive versus standing character of the system (Van Maanen et al., 2013; Ward et al., 2018; Zhou et al., 2018); and (c) the wave climate, affecting both the basin hydrodynamics and its sediment transport regime (Carniello et al., 2011; A. D'Alpaos et al., 2013). Particularly important is the spatial distribution of salt marshes within the back-barrier basin. As demonstrated by Donatelli et al. (2020b), different hydrodynamic changes due to marsh loss are to be expected in back-barrier systems where most marshes fringe the mainland compared to those characterized by the presence of extensive marsh areas detached from the mainland.

Second, our simulated scenarios do not account for salt-marsh landward migration, which can mitigate the net loss of salt marshes (e.g., Enwright et al., 2016; Fagherazzi et al., 2019; Feagin et al., 2010; Field et al., 2016; Kirwan & Gedan, 2019). Even though this process is typically hindered by the presence of levees and dikes at the interface between marshes and the upland (e.g., Yang et al., 2022), it cannot be disregarded a priori. The colonization of new intertidal areas by marsh upland migration would profoundly change the hydrodynamics and sediment budget of the whole back-barrier system, as new areas would be periodically flooded by tides and additional sediment volumes would become available as marshes expand landward.

Finally, the timescale required for the system to morphodynamically adapt to changes in marsh coverage is generally difficult to quantify. This is because sediment volumes made available by marsh lateral erosion can be redistributed within the basin, thus affecting both the net sediment budget and the related morphological changes (Donatelli, Kalra, et al., 2020; Eelsey-Quirk et al., 2019; Kalra et al., 2021). In our simulations, sediments eroded from marshes are instantaneously removed and can no longer contribute to the lagoon's morphological evolution. Moreover, it should be noted that salt-marsh loss seldom occurs without inducing modifications to other back-barrier landforms. This is clearly highlighted by historical field data from the Venice Lagoon, which suggests mutual feedback between marsh erosion and tidal-flat deepening. Therefore, generalizations of results obtained from hypothetical erosive scenarios should be treated with caution, since the modeled hydrodynamic changes could be mitigated or magnified by other morphodynamic adjustments induced by marsh disappearance on the tidal back-barrier system as a whole.

In view of the above, the effects of salt-marsh loss on the hydrodynamic and morphodynamics of shallow back-barrier tidal systems are likely to be extremely site-specific, and therefore difficult to generalize. Moreover, biogeomorphological feedbacks, which are key drivers of marsh spatiotemporal evolution, are likely to vary geographically as a consequence of distinct ecological community assemblages and different climatic forcings. This further complicates predicting the morphodynamic effects of salt-marsh loss, as well as the timescales over which such effects would manifest (Bertness & Ewanchuk, 2002; Finotello, D'Alpaos et al., 2022; Pennings & He, 2021; Wilson et al., 2022).

6. Conclusions

In this study, we focused on the microtidal Venice Lagoon (Italy) to disentangle the role played by the loss of salt marshes on the hydrodynamics of tidal back-barrier embayments. Numerical simulations were performed

considering both past morphological configurations of the lagoon dating back up to 1887 and hypothetical scenarios involving additional marsh erosion relative to the present-day conditions. This allowed us to highlight both the direct and indirect effects of salt-marsh loss on the evolution of the lagoon hydrodynamics. Direct effects include enhanced mean-high water levels due to reduced energy dissipation at high-water stages, and the formation of higher and more powerful wind waves due to longer fetches. Moreover, historical data and numerical results suggest that marsh disappearance is likely to trigger tidal-flat deepening, thus leading to increased tidal ranges due to reduced energy dissipation and modifications of local tidal asymmetries. We also speculated on the potential impacts of the observed hydrodynamic changes on the lagoon ecomorphodynamic evolution, as well as on the associated risk of tidal flooding in urban settlements. Our analyses suggest that a failure to restore and protect the existing marshes in the past would have not critically affected the flooding risk in urban lagoonal settlements. On the contrary, flooding risk would have been significantly increased in the lagoon marginal areas, mostly due to larger wave heights. Our findings provide novel insights into the hydrodynamic effects of salt-marsh loss in sediment-starving, shallow tidal embayments morphodynamically dominated by wind-driven sediment transport processes, with far-reaching implications for the conservation and restoration of coastal ecosystems that extend well beyond the study case at hand. However, we stress that care should be given to generalizing the results presented here to tidal embayments that are morphologically and morphodynamically different from the Venice Lagoon. We support the idea that the response of back-barrier systems to changing external forcing is highly dependent on site-specific morphological and ecological features, as well as on the site-specific characteristics of tides, waves, and sediments.

Data Availability Statement

All data needed to evaluate the results presented in the paper can be found at <http://researchdata.cab.unipd.it/id/eprint/646>. Meteorological data for the Venice Lagoon are also freely available at www.comune.venezia.it/content/dati-dalle-stazioni-rilevamento and www.venezia.isprambiente.it/rete-meteo-mareografica. Data regarding the morphology of the Venice Lagoon, including those related to salt-marsh coverage, can be found at <http://www.atlantedelalaguna.it/>.

Acknowledgments

This scientific activity was performed in the framework of the Research Programme Venezia2021, with the contribution of the Provveditorato for the Public Works of Veneto, Trentino Alto Adige, and Friuli Venezia Giulia, provided through the concessionary of State Consorzio Venezia Nuova and coordinated by CORILA, Research Line 3.2 (PI Andrea D'Alpaos). The authors are grateful for constructive comments from Carmine Donatelli and two anonymous reviewers. Open Access Funding provided by Università degli Studi di Padova within the CRUI-CARE Agreement.

References

- Allen, J. I., Somerfield, P. J., & Gilbert, F. J. (2007). Quantifying uncertainty in high-resolution coupled hydrodynamic-ecosystem models. *Journal of Marine Systems*, 64(1–4), 3–14. <https://doi.org/10.1016/j.jmarsys.2006.02.010>
- Amos, C. L., Umgiesser, G., Tosi, L., & Townend, I. H. (2010). The coastal morphodynamics of Venice lagoon, Italy: An introduction. *Continental Shelf Research*, 30(8), 837–846. <https://doi.org/10.1016/j.csr.2010.01.014>
- Aubrey, D. G., & Speer, P. E. (1985). A study of non-linear tidal propagation in shallow inlet/estuarine systems Part I: Observations. *Estuarine, Coastal and Shelf Science*, 21(2), 185–205. [https://doi.org/10.1016/0272-7714\(85\)90096-4](https://doi.org/10.1016/0272-7714(85)90096-4)
- Barausse, A., Grechi, L., Martinello, N., Musner, T., Smania, D., Zangaglia, A., & Palmeri, L. (2015). An integrated approach to prevent the erosion of salt marshes in the lagoon of Venice. *EQA - International Journal of Environmental Quality*, 18(1), 43–54. <https://doi.org/10.6092/issn.2281-4485/5799>
- Barbier, E. B. E. B., Hacker, S. D. S. D., Kennedy, C., Koch, E. W. E. W., Stier, A. C. A. C., & Silliman, B. R. B. R. (2011). The value of estuarine and coastal ecosystem services. *Ecological Monographs*, 81(2), 169–193. <https://doi.org/10.1890/10.1510.1>
- Bertness, M. D., & Ewanchuk, P. J. (2002). Latitudinal and climate-driven variation in the strength and nature of biological interactions in New England salt marshes. *Oecologia*, 132(3), 392–401. <https://doi.org/10.1007/s00442-002-0972-y>
- Boothroyd, J. C., Friedrich, N. E., & McGinn, S. R. (1985). Geology of microtidal coastal lagoons: Rhode Island. *Marine Geology*, 63(1–4), 35–76. [https://doi.org/10.1016/0025-3227\(85\)90079-9](https://doi.org/10.1016/0025-3227(85)90079-9)
- Carbognin, L., Teatini, P., & Tosi, L. (2004). Eustacy and land subsidence in the Venice Lagoon at the beginning of the new millennium. *Journal of Marine Systems*, 51(1–4 SPEC. ISS), 345–353. <https://doi.org/10.1016/j.jmarsys.2004.05.021>
- Carniello, L., D'Alpaos, A., Botter, G., & Rinaldo, A. (2016). Statistical characterization of spatiotemporal sediment dynamics in the Venice lagoon. *Journal of Geophysical Research F: Earth Surface*, 121(5), 1049–1064. <https://doi.org/10.1002/2015JF003793>
- Carniello, L., D'Alpaos, A., & Defina, A. (2011). Modeling wind waves and tidal flows in shallow micro-tidal basins. *Estuarine, Coastal and Shelf Science*, 92(2), 263–276. <https://doi.org/10.1016/j.ecss.2011.01.001>
- Carniello, L., D'Alpaos, L., Defina, A., & Fagherazzi, S. (2008). A conceptual model for the long term evolution of tidal flats in the Venice lagoon. *River, Coastal and Estuarine Morphodynamics: RCEM 2007 - Proceedings of the 5th IAHR Symposium on River, Coastal and Estuarine Morphodynamics*, 1, 137–144. <https://doi.org/10.1201/noe0415453639-c18>
- Carniello, L., Defina, A., & D'Alpaos, L. (2009). Morphological evolution of the Venice lagoon: Evidence from the past and trend for the future. *Journal of Geophysical Research*, 114(4), 1–10. <https://doi.org/10.1029/2008JF001157>
- Carniello, L., Defina, A., & D'Alpaos, L. (2012). Modeling sand-mud transport induced by tidal currents and wind waves in shallow microtidal basins: Application to the Venice Lagoon (Italy). *Estuarine, Coastal and Shelf Science*, 102–103, 105–115. <https://doi.org/10.1016/j.ecss.2012.03.016>
- Carniello, L., Defina, A., Fagherazzi, S., & D'Alpaos, L. (2005). A combined wind wave-tidal model for the Venice lagoon, Italy. *Journal of Geophysical Research*, 110(4), 1. <https://doi.org/10.1029/2004JF000232>
- Carniello, L., Silvestri, S., Marani, M., D'Alpaos, A., Volpe, V., & Defina, A. (2014). Sediment dynamics in shallow tidal basins: In situ observations, satellite retrievals, and numerical modeling in the Venice Lagoon. *Journal of Geophysical Research: Earth Surface*, 119(4), 802–815. <https://doi.org/10.1002/2013JF003015>

- Chmura, G. L., Anisfeld, S. C., Cahoon, D. R., & Lynch, J. C. (2003). Global carbon sequestration in tidal, saline wetland soils. *Global Biogeochemical Cycles*, 17(4), 21. <https://doi.org/10.1029/2002gb001917>
- Costanza, R., D'Arge, R., De Groot, R., Farber, S., Grasso, M., Hannon, B., et al. (1997). The value of the world's ecosystem services and natural capital. *Nature*, 387(6630), 253–260. <https://doi.org/10.1038/387253a0>
- D'Alpaos, A., Carniello, L., & Rinaldo, A. (2013). Statistical mechanics of wind wave-induced erosion in shallow tidal basins: Inferences from the Venice Lagoon. *Geophysical Research Letters*, 40(13), 3402–3407. <https://doi.org/10.1002/grl.50666>
- D'Alpaos, A., Lanzoni, S., Marani, M., & Rinaldo, A. (2007). Landscape evolution in tidal embayments: Modeling the interplay of erosion, sedimentation, and vegetation dynamics. *Journal of Geophysical Research*, 112(1), 1–17. <https://doi.org/10.1029/2006JF000537>
- D'Alpaos, A., Lanzoni, S., Marani, M., & Rinaldo, A. (2009). On the O'Brien-Jarrett-Marchi law. *Rendiconti Lincei*, 20(3), 225–236. <https://doi.org/10.1007/s12210-009-0052-x>
- D'Alpaos, C., & D'Alpaos, A. (2021). The valuation of ecosystem services in the Venice lagoon: A multicriteria approach. *Sustainability*, 13(17), 9485. <https://doi.org/10.3390/su13179485>
- D'Alpaos, L. (2010). In L. D'Alpaos (Ed.), *Fatti e misfatti di idraulica lagunare. La laguna di Venezia dalla diversione dei fiumi alle nuove opere delle bocche di porto*, Istituto Veneto di Scienze, Lettere e Arti (Vol. 1999). Istituto Veneto di Scienze, Lettere ed Arti.
- D'Alpaos, L., & Martini, P. (2005). The influence of the inlet configuration on sediment loss in the Venice Lagoon. In C. A. Fletcher & T. Spencer (Eds.), *Flooding and environmental challenges for Venice and its lagoon: State of knowledge* (p. 691). Cambridge University Press.
- Deb, M., Abdolali, A., Kirby, J. T., Shi, F., Guiteras, S., & McDowell, C. (2022). Sensitivity of tidal hydrodynamics to varying bathymetric configurations in a multi-inlet rapidly eroding salt marsh system: A numerical study. *Earth Surface Processes and Landforms*, 47(5), 1157–1182. <https://doi.org/10.1002/esp.5308>
- Defina, A. (2000). Two-dimensional shallow flow equations for partially dry areas. *Water Resources Research*, 36(11), 3251–3264. <https://doi.org/10.1029/2000WR900167>
- Defina, A., Carniello, L., Fagherazzi, S., & D'Alpaos, L. (2007). Self-organization of shallow basins in tidal flats and salt marshes. *Journal of Geophysical Research*, 112(3), 1–11. <https://doi.org/10.1029/2006JF000550>
- De Swart, H. E., & Zimmerman, J. T. F. (2009). Morphodynamics of tidal inlet systems. *Annual Review of Fluid Mechanics*, 41(1), 203–229. <https://doi.org/10.1146/annurev.fluid.010908.165159>
- Donatelli, C., Ganju, N. K., Zhang, X., Fagherazzi, S., & Leonardi, N. (2018). Salt marsh loss affects tides and the sediment budget in shallow bays. *Journal of Geophysical Research: Earth Surface*, 123(10), 2647–2662. <https://doi.org/10.1029/2018JF004617>
- Donatelli, C., Kalra, T. S., Fagherazzi, S., Zhang, X., & Leonardi, N. (2020). Dynamics of marsh-derived sediments in lagoon-type estuaries. *Journal of Geophysical Research: Earth Surface*, 125(12). <https://doi.org/10.1029/2020JF005751>
- Donatelli, C., Zhang, X., Ganju, N. K., Aretxabaleta, A. L., Fagherazzi, S., & Leonardi, N. (2020). A nonlinear relationship between marsh size and sediment trapping capacity compromises salt marshes' stability. *Geology*, 48(10), 966–970. <https://doi.org/10.1130/G47131.1>
- Dronkers, J. (1986). Tidal asymmetry and estuarine morphology. *Netherlands Journal of Sea Research*, 20(2–3), 117–131. [https://doi.org/10.1016/0077-7579\(86\)90036-0](https://doi.org/10.1016/0077-7579(86)90036-0)
- Duran Vinent, O., Herbert, E. R., Coleman, D. J., Himmelstein, J. D., & Kirwan, M. L. (2021). Onset of runaway fragmentation of salt marshes. *One Earth*, 4(4), 506–516. <https://doi.org/10.1016/j.oneear.2021.02.013>
- Elsley-Quirk, T., Mariotti, G., Valentine, K., & Raper, K. (2019). Retreating marsh shoreline creates hotspots of high-marsh plant diversity. *Scientific Reports*, 9(1), 1–9. <https://doi.org/10.1038/s41598-019-42119-8>
- Enwright, N. M., Griffith, K. T., & Osland, M. J. (2016). Barriers to and opportunities for landward migration of coastal wetlands with sea-level rise. *Frontiers in Ecology and the Environment*, 14(6), 307–316. <https://doi.org/10.1002/fee.1282>
- Fagherazzi, S., Anisfeld, S. C., Blum, L. K., Long, E. V., Feagin, R. A., Fernandes, A., et al. (2019). Sea level rise and the dynamics of the marsh-upland boundary. *Frontiers in Environmental Science*, 7(FEB), 1–18. <https://doi.org/10.3389/fenvs.2019.00025>
- Fagherazzi, S., Carniello, L., D'Alpaos, L., & Defina, A. (2006). Critical bifurcation of shallow microtidal landforms in tidal flats and salt marshes. *Proceedings of the National Academy of Sciences of the United States of America*, 103(22), 8337–8341. <https://doi.org/10.1073/pnas.0508379103>
- Fagherazzi, S., Kirwan, M. L., Mudd, S. M., Guntenspergen, G. R., Temmerman, S., D'Alpaos, A., et al. (2012). Numerical models of salt marsh evolution: Ecological, geomorphic, and climatic factors. *Reviews of Geophysics*, 50(1), 1–28. <https://doi.org/10.1029/2011RG000359>
- Feagin, R. A., Martinez, M. L., Mendoza-Gonzalez, G., & Costanza, R. (2010). Salt marsh zonal migration and ecosystem service change in response to global sea level rise: A case study from an urban region. *Ecology and Society*, 15(4), art14. <https://doi.org/10.5751/ES-03724-150414>
- Ferrarin, C., Tomasin, A., Bajo, M., Petrizzo, A., & Umgiesser, G. (2015). Tidal changes in a heavily modified coastal wetland. *Continental Shelf Research*, 101, 22–33. <https://doi.org/10.1016/j.csr.2015.04.002>
- Ferrighi, A. (2005). In C. A. Fletcher & T. Spencer (Eds.), *Flooding and environmental challenges for Venice and its lagoon: State of knowledge*. Cambridge University Press.
- Field, C. R., Gjerdrum, C., & Elphick, C. S. (2016). Forest resistance to sea-level rise prevents landward migration of tidal marsh. *Biological Conservation*, 201, 363–369. <https://doi.org/10.1016/j.biocon.2016.07.035>
- Finkelstein, K., & Ferland, M. A. (1987). Back-barrier response to sea-level rise, eastern shore of Virginia. *Sea-Level Fluctuation and Coastal Evolution*, 145–155. <https://doi.org/10.2110/pec.87.41.0145>
- Finotello, A., Canestrelli, A., Carniello, L., Ghinassi, M., & D'Alpaos, A. (2019). Tidal flow asymmetry and discharge of lateral tributaries drive the evolution of a microtidal meander in the Venice Lagoon (Italy). *Journal of Geophysical Research: Earth Surface*, 124(12), 3043–3066. <https://doi.org/10.1029/2019JF005193>
- Finotello, A., Capperucci, R. M., Bartholomä, A., D'Alpaos, A., & Ghinassi, M. (2022). Morpho-sedimentary evolution of a microtidal meandering channel driven by 130 years of natural and anthropogenic modifications of the Venice Lagoon (Italy). *Earth Surface Processes and Landforms*, 47(10), 2580–2596. <https://doi.org/10.1002/esp.5396>
- Finotello, A., D'Alpaos, A., Marani, M., & Bertuzzo, E. (2022). A minimalist model of salt-marsh vegetation dynamics driven by species competition and dispersal. *Frontiers in Marine Science*, 9(866570), 1–23. <https://doi.org/10.3389/fmars.2022.866570>
- Finotello, A., Marani, M., Carniello, L., Pivato, M., Roner, M., Tommasini, L., & D'Alpaos, A. (2020). Control of wind-wave power on morphological shape of salt marsh margins. *Water Science and Engineering*, 13(1), 45–56. <https://doi.org/10.1016/j.wse.2020.03.006>
- Fitzgerald, D. M., & Hughes, Z. (2019). Marsh processes and their response to climate change and sea-level rise. *Annual Review of Earth and Planetary Sciences*, 47(1), 481–517. <https://doi.org/10.1146/annurev-earth-082517-010255>
- Flemming, B. W. (2012). Geology, morphology, and sedimentology of estuaries and coasts. *Treatise on Estuarine and Coastal Science*, 3, 7–38. <https://doi.org/10.1016/B978-0-12-374711-2.00302-8>
- Fortunato, A. B., & Oliveira, A. (2005). Influence of intertidal flats on tidal asymmetry. *Journal of Coastal Research*, 21(5), 1062–1067. <https://doi.org/10.2112/03-0089.1>

- Friedrichs, C. T. (2012). Tidal flat morphodynamics: A synthesis. *Treatise on Estuarine and Coastal Science*, 3, 137–170. <https://doi.org/10.1016/B978-0-12-374711-2.00307-7>
- Gambolati, G., & Teatini, P. (2014). Anthropogenic uplift of Venice by using seawater. *Venice Shall Rise Again*, 57–77. <https://doi.org/10.1016/b978-0-12-420144-6.00005-4>
- Gatto, P., & Carbognin, L. (1981). The lagoon of Venice: Natural environmental trend and man-induced modification. *Hydrological Sciences Bulletin*, 26(4), 379–391. <https://doi.org/10.1080/02626668109490902>
- Ghezzi, M., Guerzoni, S., Cucco, A., & Umgiesser, G. (2010). Changes in Venice Lagoon dynamics due to construction of mobile barriers. *Coastal Engineering*, 57(7), 694–708. <https://doi.org/10.1016/j.coastaleng.2010.02.009>
- Gilby, B. L., Weinstein, M. P., Baker, R., Cebrian, J., Alford, S. B., Chelsky, A., et al. (2021). Human actions alter tidal marsh seascapes and the provision of ecosystem services. *Estuaries and Coasts*, 44(6), 1628–1636. <https://doi.org/10.1007/s12237-020-00830-0>
- González-Villanueva, R., Pérez-Arlucea, M., Costas, S., Bao, R., Otero, X. L., & Goble, R. (2015). 8000 years of environmental evolution of barrier-lagoon systems emplaced in coastal embayments (NW Iberia). *The Holocene*, 25(11), 1786–1801. <https://doi.org/10.1177/0959683615591351>
- Gourgue, O., Van Belzen, J., Schwarz, C., Vandembrouwaene, W., Vanlede, J., Belliard, J. P., et al. (2022). Biogeomorphic modeling to assess the resilience of tidal-marsh restoration to sea level rise and sediment supply. *Earth Surface Dynamics*, 10(3), 531–553. <https://doi.org/10.5194/esurf-10-531-2022>
- Green, M. O., & Coco, G. (2014). Review of wave-driven sediment resuspension and transport in estuaries. *Reviews of Geophysics*, 52(1), 77–117. <https://doi.org/10.1002/2013RG000437>
- Guo, L., Wang, Z. B., Townend, I., & He, Q. (2019). Quantification of tidal asymmetry and its nonstationary variations. *Journal of Geophysical Research: Oceans*, 124(1), 773–787. <https://doi.org/10.1029/2018JC014372>
- Hesp, P. A. (2016). Coastal barriers. In M. J. Kennish (Ed.), *Encyclopedia of Earth sciences series* (pp. 128–130). Springer Netherlands. https://doi.org/10.1007/978-94-017-8801-4_279
- Holthuijsen, L. H., Booij, N., & Herbers, T. H. C. (1989). A prediction model for stationary, short-crested waves in shallow water with ambient currents. *Coastal Engineering*, 13(1), 23–54. [https://doi.org/10.1016/0378-3839\(89\)90031-8](https://doi.org/10.1016/0378-3839(89)90031-8)
- Hopkinson, C. S., Wolanski, E., Cahoon, D. R., Perillo, G. M. E., & Brinson, M. M. (2018). Coastal wetlands: A synthesis. In G. Perillo, E. Wolanski, D. R. Cahoon, & C. S. Hopkinson (Eds.), *Coastal wetlands: An integrated ecosystem approach* (pp. 1–75). Elsevier. <https://doi.org/10.1016/B978-0-444-63893-9.00001-0>
- Hughes, Z. J., FitzGerald, D. M., & Wilson, C. A. (2021). Impacts of climate change and sea level rise. In D. M. FitzGerald & Z. J. Hughes (Eds.), *Salt marshes* (pp. 476–481). Cambridge University Press. <https://doi.org/10.1017/9781316888933.021>
- Jarrett, J. T. (1976). Tidal prism - Inlet area relationships (general investigation of tidal inlets, report 3). *Journal of Waterways and Harbors*, 95, 55.
- Kalra, T. S., Ganju, N. K., Aretxabaleta, A. L., Carr, J. A., Defne, Z., & Moriarty, J. M. (2021). Modeling marsh dynamics using a 3-D coupled wave-flow-sediment model. *Frontiers in Marine Science*, 8(November). <https://doi.org/10.3389/fmars.2021.740921>
- Kirwan, M. L., & Gedan, K. B. (2019). Sea-level driven land conversion and the formation of ghost forests. *Nature Climate Change*, 9(6), 450–457. <https://doi.org/10.1038/s41558-019-0488-7>
- Kjerfve, B. (1994). Coastal lagoons. In M. J. Kennish (Ed.), *Encyclopedia of estuaries* (pp. 140–143). Springer Netherlands. https://doi.org/10.1007/978-94-017-8801-4_47
- Leonardi, N., Defne, Z., Ganju, N. K., & Fagherazzi, S. (2016). Salt marsh erosion rates and boundary features in a shallow Bay. *Journal of Geophysical Research: Earth Surface*, 121(10), 1861–1875. <https://doi.org/10.1002/2016JF003975>
- Leonardi, N., Ganju, N. K., & Fagherazzi, S. (2016). A linear relationship between wave power and erosion determines salt-marsh resilience to violent storms and hurricanes. *Proceedings of the National Academy of Sciences of the United States of America*, 113(1), 64–68. <https://doi.org/10.1073/pnas.1510095112>
- Levin, L. A., Boesch, D. F., Covich, A., Dahm, C., Eerséus, C., Ewel, K. C., et al. (2001). The function of marine critical transition zones and the importance of sediment biodiversity. *Ecosystems*, 4(5), 430–451. <https://doi.org/10.1007/s10021-001-0021-4>
- Marani, M., D'Alpaos, A., Lanzoni, S., & Santalucia, M. (2011). Understanding and predicting wave erosion of marsh edges. *Geophysical Research Letters*, 38(21), 1. <https://doi.org/10.1029/2011GL048995>
- Marani, M., D'alpaos, A., Lanzoni, S., & Santalucia, M. (2011). Understanding and predicting wave erosion of marsh edges. *Geophysical Research Letters*, 38(21). <https://doi.org/10.1029/2011GL048995>
- Mariotti, G. (2020). Beyond marsh drowning: The many faces of marsh loss (and gain). *Advances in Water Resources*, 144(April), 103710. <https://doi.org/10.1016/j.advwatres.2020.103710>
- Mariotti, G., & Fagherazzi, S. (2010). A numerical model for the coupled long-term evolution of salt marshes and tidal flats. *Journal of Geophysical Research*, 115(1), F01004. <https://doi.org/10.1029/2009JF001326>
- Mariotti, G., & Fagherazzi, S. (2013). Critical width of tidal flats triggers marsh collapse in the absence of sea-level rise. *Proceedings of the National Academy of Sciences of the United States of America*, 110(14), 5353–5356. <https://doi.org/10.1073/pnas.1219600110>
- Matticchio, B., Carniello, L., Canesso, D., Ziggio, E., & Cordella, M. (2017). Recent changes in tidal propagation in the Venice Lagoon: Effects of changes in the inlet structure. In L. D'Alpaos (Ed.), *Commissione di studio sui problemi di Venezia, volume III: La laguna di Venezia e le nuove opere alle bocche (Istituto V, pp. 157–183)*. Istituto Veneto di Scienze, Lettere ed Arti.
- Mcowen, C. J., Weatherdon, L. V., Van Bochove, J. W., Sullivan, E., Blyth, S., Zockler, C., et al. (2017). A global map of saltmarshes. *Biodiversity Data Journal*, 5(1), e11764. <https://doi.org/10.3897/BDJ.5.e11764>
- Mel, R. A., Bandoni, M., & Steffinlongo, D. (2022). Salt-marsh retreat on different time scales: Issues and prospects from a 5-year monitoring campaign in the Venice Lagoon. *Earth Surface Processes and Landforms*, 47(8), 1989–2005. <https://doi.org/10.1002/esp.5359>
- Mel, R. A., Carniello, L., & D'Alpaos, L. (2021). How long the Mo.S.E. Barriers will be effective in protecting all urban settlements within the Venice lagoon? The wind setup constraint. *Coastal Engineering*, 168(January), 103923. <https://doi.org/10.1016/j.coastaleng.2021.103923>
- Mel, R. A., Viero, D. P., Carniello, L., Defina, A., & D'Alpaos, L. (2021). The first operations of Mo.S.E. system to prevent the flooding of Venice: Insights on the hydrodynamics of a regulated lagoon. *Estuarine, Coastal and Shelf Science*, 261(August), 107547. <https://doi.org/10.1016/j.ecss.2021.107547>
- Möller, I., Kudella, M., Rupprecht, F., Spencer, T., Paul, M., Van Wesenbeeck, B. K., et al. (2014). Wave attenuation over coastal salt marshes under storm surge conditions. *Nature Geoscience*, 7(10), 727–731. <https://doi.org/10.1038/NNGEO2251>
- Murty, T. S. (1990). Nonlinear tidal distortion in shallow well-mixed estuaries. *Estuarine, Coastal and Shelf Science*, 30(3), 321–322. [https://doi.org/10.1016/0272-7714\(90\)90054-U](https://doi.org/10.1016/0272-7714(90)90054-U)
- Nelson, J. L., & Zavaleta, E. S. (2012). Salt marsh as a coastal filter for the oceans: Changes in function with experimental increases in Nitrogen loading and sea-level rise. *PLoS One*, 7(8), e38558. <https://doi.org/10.1371/journal.pone.0038558>
- Nidzicko, N. J. (2010). Tidal asymmetry in estuaries with mixed semidiurnal/diurnal tides. *Journal of Geophysical Research*, 115(8), 1–13. <https://doi.org/10.1029/2009JC005864>

- Orton, P. M., Sanderson, E. W., Talke, S. A., Giampieri, M., & MacManus, K. (2020). Storm tide amplification and habitat changes due to urbanization of a lagoonal estuary. *Natural Hazards and Earth System Sciences*, 20(9), 2415–2432. <https://doi.org/10.5194/nhess-20-2415-2020>
- Passeri, D. L., Dalyander, P. S., Long, J. W., Mickey, R. C., Jenkins, R. L., Thompson, D. M., et al. (2020). The roles of storminess and sea level rise in decadal barrier island evolution. *Geophysical Research Letters*, 47(18), e2020GL089370. <https://doi.org/10.1029/2020GL089370>
- Pennings, S. C., & He, Q. (2021). Community ecology of salt marshes. In D. M. FitzGerald & Z. J. Hughes (Eds.), *Salt marshes* (pp. 82–112). Cambridge University Press. <https://doi.org/10.1017/9781316888933.006>
- Pérez-Ruzafa, A., Pérez-Ruzafa, I. M., Newton, A., & Marcos, C. (2019). Coastal Lagoons: Environmental variability, ecosystem complexity, and goods and services uniformity. In E. Wolanski, J. W. Day, M. Elliott, & R. Ramachandran (Eds.), *Coasts and estuaries: The future* (pp. 253–276). Elsevier. <https://doi.org/10.1016/B978-0-12-814003-1.00015-0>
- Perillo, G. M. E. (1995). Chapter 1: Geomorphology and sedimentology of estuaries: An introduction. In *Gerardo miguel eduardo perillo. In Developments in sedimentology* (Vol. 53, pp. 1–16). Elsevier. [https://doi.org/10.1016/S0070-4571\(05\)80021-4](https://doi.org/10.1016/S0070-4571(05)80021-4)
- Pollard, J. A., Spencer, T., & Brooks, S. M. (2019). The interactive relationship between coastal erosion and flood risk. *Progress in Physical Geography*, 43(4), 574–585. <https://doi.org/10.1177/0309133318794498>
- Ralston, D. K., Talke, S., Geyer, W. R., Al-Zubaidi, H. A. M., & Sommerfield, C. K. (2019). Bigger tides, less flooding: Effects of dredging on barotropic dynamics in a highly modified estuary. *Journal of Geophysical Research: Oceans*, 124(1), 196–211. <https://doi.org/10.1029/2018JC014313>
- Rinaldo, A., Fagherazzi, S., Lanzoni, S., Marani, M., & Dietrich, W. E. (1999). Tidal networks 3. Landscape-forming discharges and studies in empirical geomorphic relationships. *Water Resources Research*, 35(12), 3919–3929. <https://doi.org/10.1029/1999WR900238>
- Rinaldo, A., Nicotina, L., Alessi Celegon, E., Beraldin, F., Botter, G., Carniello, L., et al. (2008). Sea level rise, hydrologic runoff, and the flooding of Venice. *Water Resources Research*, 44(12), 1–12. <https://doi.org/10.1029/2008WR007195>
- Ruol, P., Favaretto, C., Volpato, M., & Martinelli, L. (2020). Flooding of Piazza san Marco (Venice): Physical model tests to evaluate the overtopping discharge. *Water (Switzerland)*, 12(2), 427. <https://doi.org/10.3390/w12020427>
- Silvestri, S., D'Alpaos, A., Nordio, G., & Carniello, L. (2018). Anthropogenic modifications can significantly influence the local mean sea level and affect the survival of salt marshes in shallow tidal systems. *Journal of Geophysical Research: Earth Surface*, 123(5), 996–1012. <https://doi.org/10.1029/2017JF004503>
- Soulsby, R. L. (1995). Bed shear-stresses due to combined waves and currents. In M. J. F. et al Stive (Ed.), *Advanced in coastal morphodynamics* (pp. 20–23). Delft Hydraulics.
- Stutz, M. L., & Pilkey, O. H. (2011). Open-ocean barrier islands: Global influence of climatic, oceanographic, and depositional settings. *Journal of Coastal Research*, 27(2), 207–222. <https://doi.org/10.2112/09-1190.1>
- Tagliapietra, D., Baldan, D., Barausse, A., Buosi, A., Curiel, D., Guarneri, I., et al. (2018). Protecting and restoring the salt marshes and seagrasses in the lagoon of Venice. In X. D. Quintana, D. Boix, S. Gascón, & J. Sala (Eds.), *Management and restoration of Mediterranean coastal Lagoons in Europe. Included in the project "LIFE pletera (LIFE13 NAT/ES/001001) (Càtedra d' p. 220). Càtedra d'Ecosistemes Litorals Mediterrànis i LIFE Pletera*. Retrieved from http://lifepletera.com/wp-content/uploads/2019/02/Recerca_i_Territori_10_ENG_MdM_web.pdf
- Tambroni, N., & Seminara, G. (2006). Are inlets responsible for the morphological degradation of Venice Lagoon? *Journal of Geophysical Research*, 111(3), 1. <https://doi.org/10.1029/2005JF000334>
- Temmerman, S., Meire, P., Bouma, T. J., Herman, P. M. J., Ysebaert, T., & De Vriend, H. J. (2013). Ecosystem-based coastal defence in the face of global change. *Nature*, 504(7478), 79–83. <https://doi.org/10.1038/nature12859>
- Tognin, D., D'Alpaos, A., Marani, M., & Carniello, L. (2021). Marsh resilience to sea-level rise reduced by storm-surge barriers in the Venice Lagoon. *Nature Geoscience*, 14(12), 906–911. <https://doi.org/10.1038/s41561-021-00853-7>
- Tognin, D., Finotello, A., D'Alpaos, A., Viero, D. P., Pivato, M., Mel, R. A., et al. (2022). Loss of geomorphic diversity in shallow tidal embayments promoted by storm-surge barriers. *Science Advances*, 8(13), 1–13. <https://doi.org/10.1126/sciadv.abm8446>
- Tomasin, A. (1974). Recent changes in the tidal regime in Venice. *Rivista Italiana Geofisica*, 23(5/6), 275–278.
- Tommasini, L., Carniello, L., Ghinassi, M., Roner, M., & D'Alpaos, A. (2019). Changes in the wind-wave field and related salt-marsh lateral erosion: Inferences from the evolution of the Venice lagoon in the last four centuries. *Earth Surface Processes and Landforms*, 44(8), 1633–1646. <https://doi.org/10.1002/esp.4599>
- Valiela, I., Kinney, E., Culbertson, J., Peacock, E., & Smith, S. (2009). Global loss of mangroves and salt marshes. In C. M. Duarte (Ed.), *Global loss of coastal habitats rates, causes and consequences (fundacion* (pp. 107–142).
- Valle-Levinson, A., Marani, M., Carniello, L., D'Alpaos, A., & Lanzoni, S. (2021). Astronomic link to anomalously high mean sea level in the northern Adriatic Sea. *Estuarine, Coastal and Shelf Science*, 257(February), 107418. <https://doi.org/10.1016/j.ecss.2021.107418>
- Van Maanen, B., Coco, G., & Bryan, K. R. (2013). Modelling the effects of tidal range and initial bathymetry on the morphological evolution of tidal embayments. *Geomorphology*, 191, 23–34. <https://doi.org/10.1016/j.geomorph.2013.02.023>
- Vinet, L., & Zhedanov, A. (2011). A "missing" family of classical orthogonal polynomials. *Journal of Physics A: Mathematical and Theoretical*, 44(8), 085201. <https://doi.org/10.1088/1751-8113/44/8/085201>
- Ward, S. L., Robins, P. E., Lewis, M. J., Iglesias, G., Hashemi, M. R., & Neill, S. P. (2018). Tidal stream resource characterisation in progressive versus standing wave systems. *Applied Energy*, 220(October), 274–285. <https://doi.org/10.1016/j.apenergy.2018.03.059>
- Wilson, C. A., Hughes, Z. J., & FitzGerald, D. M. (2022). Causal relationships among sea level rise, marsh crab activity, and salt marsh geomorphology. *Proceedings of the National Academy of Sciences of the United States of America*, 119(9), e2111535119. <https://doi.org/10.1073/pnas.2111535119>
- Yang, Z., Finotello, A., Goodwin, G., Gao, C., Mudd, S. M., Lague, D., et al. (2022). Seaward expansion of salt marshes maintains morphological self-similarity of tidal channel networks. *Journal of Hydrology*, 615(PA), 128733. <https://doi.org/10.1016/j.jhydrol.2022.128733>
- Young, I. R., & Verhagen, L. A. (1996). The growth of fetch limited waves in water of finite depth. Part 1. Total energy and peak frequency. *Coastal Engineering*, 29(1–2), 47–78. [https://doi.org/10.1016/S0378-3839\(96\)00006-3](https://doi.org/10.1016/S0378-3839(96)00006-3)
- Zanchettin, D., Bruni, S., Raichich, F., Lionello, P., Adloff, F., Androsov, A., et al. (2021). Sea-level rise in Venice: Historic and future trends (review article). *Natural Hazards and Earth System Sciences*, 21(8), 2643–2678. <https://doi.org/10.5194/nhess-21-2643-2021>
- Zarzuelo, C., López-Ruiz, A., D'Alpaos, A., Carniello, L., & Ortega-Sánchez, M. (2018). Assessing the morphodynamic response of human-altered tidal embayments. *Geomorphology*, 320, 127–141. <https://doi.org/10.1016/j.geomorph.2018.08.014>
- Zecchin, M., Baradello, L., Brancolini, G., Donda, F., Rizzetto, F., & Tosi, L. (2008). Sequence stratigraphy based on high-resolution seismic profiles in the late Pleistocene and Holocene deposits of the Venice area. *Marine Geology*, 253(3–4), 185–198. <https://doi.org/10.1016/j.margeo.2008.05.010>

- Zhou, Z., Chen, L., Townend, I., Coco, G., Friedrichs, C., & Zhang, C. (2018). Revisiting the relationship between tidal asymmetry and basin morphology: A comparison between 1D and 2D models. *Journal of Coastal Research*, 85, 151–155. <https://doi.org/10.2112/S185-031.1>
- Zhou, Z., Coco, G., Jiménez, M., Olabarrieta, M., Van Der Wegen, M., & Townend, I. (2014). Morphodynamics of river-influenced back-barrier tidal basins: The role of landscape and hydrodynamic settings. *Water Resources Research*, 50(12), 9514–9535. <https://doi.org/10.1002/2014WR015891>